

4-2014

Free-Piston Stirling Convertor Model Development, Validation, and Analysis for Space Power Systems

Jonathan F. Metscher
Embry-Riddle Aeronautical University - Daytona Beach

Follow this and additional works at: <https://commons.erau.edu/edt>



Part of the [Mechanical Engineering Commons](#)

Scholarly Commons Citation

Metscher, Jonathan F., "Free-Piston Stirling Convertor Model Development, Validation, and Analysis for Space Power Systems" (2014). *Dissertations and Theses*. 171.
<https://commons.erau.edu/edt/171>

This Thesis - Open Access is brought to you for free and open access by Scholarly Commons. It has been accepted for inclusion in Dissertations and Theses by an authorized administrator of Scholarly Commons. For more information, please contact commons@erau.edu.

Free-Piston Stirling Convertor Model Development, Validation, and Analysis for Space
Power Systems

by

Jonathan F. Metscher

A Thesis Submitted to the College of Engineering Department of Mechanical
Engineering in Partial Fulfillment of the Requirements for the Degree of
Master of Science in Mechanical Engineering

Embry-Riddle Aeronautical University
Daytona Beach, Florida
April 2014

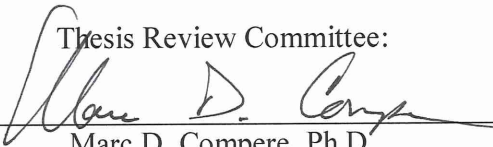
Free-Piston Stirling Converter Model Development, Validation, and Analysis for Space Power Systems

by

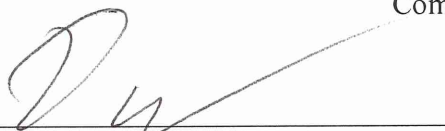
Jonathan F. Metscher

This thesis was prepared under the direction of the candidate's Thesis Committee Chair, Dr. Marc D. Compere, Assistant Professor, Daytona Beach Campus, and Thesis Committee Members Dr. Darris L. White, Professor, Daytona Beach Campus, and Dr. Edward J. Lewandowski, Project Lead Engineer, NASA Glenn Research Center, and has been approved by the Thesis Committee. It was submitted to the Department of Mechanical Engineering in partial fulfillment of the requirements for the degree of Master of Science in Mechanical Engineering


Thesis Review Committee:



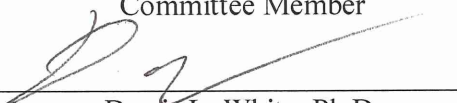
Marc D. Compere, Ph.D.
Committee Chair



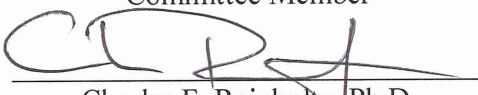
Darris L. White, Ph.D.
Committee Member



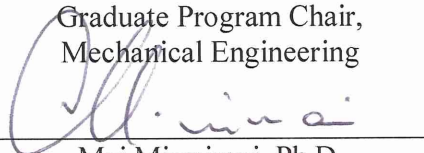
Edward J. Lewandowski, Ph.D.
Committee Member



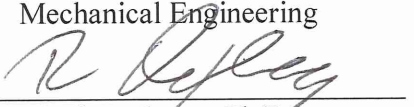
Darris L. White, Ph.D.
Graduate Program Chair,
Mechanical Engineering



Charles F. Reinholtz, Ph.D.
Department Chair,
Mechanical Engineering



Maj Mirmirani, Ph.D.
Dean, College of Engineering



Robert Oxley, Ph.D.
Associate Vice President of Academics



Date

Acknowledgements

I would like to thank Edward Lewandowski who has been my mentor and provided me the opportunity to work on a great project at NASA.

Thank you also to Steve Geng for helping me with this project and Jeff Schreiber for his review of my work. I would also like to thank the NASA Glenn Research Center Thermal Energy Conversion Branch for their support.

In addition I would like to thank Dr. Marc Compere for his input on this project in helping me through this process.

Abstract

Researcher: Jonathan F. Metscher

Title: Free-Piston Stirling Convertor Model Development, Validation, and Analysis for Space Power Systems

Institution: Embry-Riddle Aeronautical University

Degree: Master of Science in Mechanical Engineering

Year: 2014

The Advanced Stirling Convertor (ASC) is a free-piston Stirling engine coupled with a linear alternator currently being under extended testing at the NASA Glenn Research Center (GRC). Using the Sage 1-D Stirling modeling software, a linear alternator model was developed using two separate methods and integrated with an existing ASC Stirling engine model. One used a simplified transducer method, while the other was developed from first principles. The combined models were tuned and validated against test data and then compared against each other. Both validated models are able to match test data within 7% or better. In addition, a MATLAB graphical user interface (GUI) was developed to interface and operate Sage models. The GUI enables the Sage models to be run with varied input parameters, displays simulation results, and creates phasor diagrams of ASC forces and voltages. This tool also enables users with limited modeling experience to run Sage model simulations and could be useful in space mission planning.

Table of Contents

	Page
Thesis Review Committee	ii
Acknowledgements	iii
Abstract	iv
List of Tables.....	viii
List of Figures	ix
Chapter I	1
Introduction	1
A. Advanced Stirling Convertor	1
B. Linear Alternators	2
C. Statement of Problem	4
D. Thesis Statement	5
E. Limitations	5
F. Definition of Terms	5
Chapter II	7
Review of the Relevant Literature	7
A. Sage 1-D Modeling Software for Stirling Devices	7
1. Sage Description and History	7
2. Sage Model Accuracy	8
3. Sage Electromagnetic (EM) Modeling.....	9

B.	Stirling Engine and ASC Modeling.....	10
1.	Stirling Cycle Modeling and Analysis Methods.....	10
2.	Modeling of Stirling Devices with Sage	10
C.	Linear Alternator Modeling	11
1.	Magnetic Circuit Analogy (Reluctance Network)	11
D.	Summary.....	13
Chapter III.....		14
Methodology.....		14
A.	Sage Linear Alternator Modeling Using the Sage Transducer Component	14
1.	Sage Transducer Component.....	14
2.	Sage Transducer Model Circuit	15
3.	Sage transducer Model Tuning	15
B.	Sage Linear Alternator Model Using EM Components	16
1.	Sage EM Alternator Model Tuning	17
C.	Phasor Diagram Analysis of Stirling Systems	17
1.	Phasor Diagrams	17
2.	Sage/MATLAB Interface	18
3.	MATLAB GUI	19
Chapter IV.....		21

Results	21
A. Sage ASC with Transducer Alternator Results	21
1. Results at EOM/BOM Operating Conditions	21
2. Results from GRC Performance Map	21
B. Sage ASC with EM Alternator Model Results	23
1. Results at EOM/BOM Operating Conditions	23
2. Results from GRC Performance Map	24
C. Sage Alternator Comparison	26
Chapter V	28
Discussion	28
Conclusions	28
Recommendations	29
References	30
Appendices	
A First Conference Paper	33
B Second Conference Paper	45

List of Tables

	Page
Table	
Table 1. Transducer Model Results vs. Sunpower Data.....	21
Table 2. EM Model Results vs. Sunpower Data.	24

List of Figures

	Page
Figure	
<i>Figure 1.</i> ASC Cross Section	2
<i>Figure 2.</i> 2-D Cross Section of a Linear Alternator	3
<i>Figure 3.</i> Sage GUI Compents	8
<i>Figure 4.</i> Magnetic Circuit Analogy	12
<i>Figure 5.</i> Sage Transducer Component	15
<i>Figure 6.</i> Sage Transducer Alternator Model.	15
<i>Figure 7.</i> Generic Linear Alternator Diagram	16
<i>Figure 8.</i> Sage EM Alternator Model Structure.....	17
<i>Figure 9.</i> Sinusoidal Piston Forces Diagram.	18
<i>Figure 10.</i> Phasor Diagram of Piston Forces.....	18
<i>Figure 11.</i> Diagram of MATLAB and Sage Interaction	19
<i>Figure 12.</i> MATLAB GUI with Phasor Diagrams.....	20
<i>Figure 13.</i> Transducer Model Performance Map Comparison of Convertor Efficiency ..	22
<i>Figure 14.</i> Transducer Model Performance Map Comparison of Power Output	23
<i>Figure 15.</i> EM Model Performance Map Comparison of Convertor Efficiency.	25
<i>Figure 16.</i> EM Model Performance Map Comparison of Power Output	26
<i>Figure 17.</i> Alternator Model Comparison of Efficiency Results.....	27
<i>Figure 18.</i> Alternator Model Comparison of Power Output Results	27

Chapter I

Introduction

Radioisotope power systems have powered space missions to the outer planets of our solar system since the 1960s. At the more distant reaches of space the intensity of Sun light, which is inversely proportional to distance to the Sun, decreases significantly. Larger solar power systems are required to accommodate mission requirements at these distances, increasing size and mass to unacceptable limits. Radioisotope power systems offer increased power density for these missions. [1]

Current NASA deep space missions rely on radioisotope thermoelectric generators (RTGs) to supply power to spacecraft and planetary landers. RTGs supply power by converting heat from radioactive decay of Plutonium-238 into electric power with an efficiency of 5-7%. Free-piston Stirling convertors could potentially be used as a higher-efficiency alternative to RTGs, reducing the amount radioactive material used in space power systems by a factor of four. [2, 3]

A. Advanced Stirling Convertor

The Advanced Stirling Convertor (ASC), developed by Sunpower, Inc., is a free-piston Stirling engine coupled with a linear alternator and is currently under test at NASA Glenn Research Center (GRC). The ASC consists of a helium filled pressure vessel containing a piston, displacer, and linear alternator as shown in Figure 1.

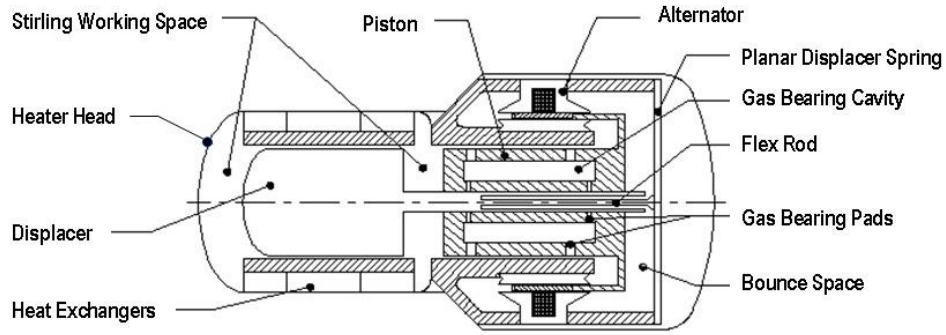


Figure 1. ASC Cross Section. Key component of the ASC are displayed in this 2-D layout.

A temperature difference across the working space creates a pressure difference, forcing the displacer to oscillate and shuttle the working fluid (helium) through the heat exchangers and regenerator. This oscillating pressure wave also creates a force on the piston forcing it into the bounce space. The displacer is connected to a planar spring in the bounce space, providing a restoring force. Magnets attached to the piston pass through the alternator in the bounce space, inducing a voltage in the alternator coil. The ASC components are designed to continually oscillate at the system's resonant frequency.

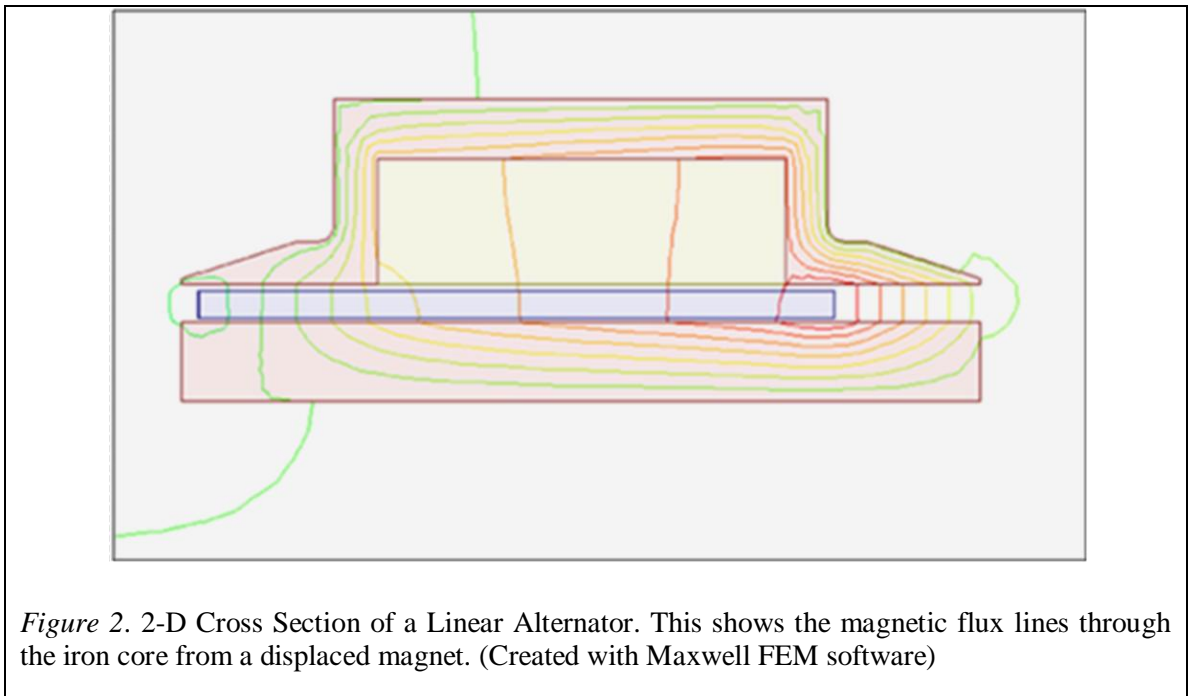
B. Linear Alternators

Alternators convert mechanical energy to electrical energy based on the principle of Faraday's Law in which a changing magnetic flux through the alternator coil induces an electromotive force (emf), or voltage (V_{emf}), in the coil. Equation (1) shows the induced voltage as the number of turns of the alternator coil (N) multiplied by the rate of change of magnetic flux. Magnetic flux (ϕ) is the integral of the magnetic field through a surface as shown in Eq. (2), where \vec{B} is the magnetic field, \hat{n} is the unit normal vector, and $d\mathbf{a}$ is the differential area element. Linear alternators, such as that in the ASC, convert the linear oscillatory motion of the piston into AC electrical power.

$$V_{emf} = -N \frac{d\phi}{dt} \quad (1)$$

$$\phi = \int \vec{B} \cdot \hat{n} \, d\mathbf{a} \quad (2)$$

Linear alternators configurations are divided into categories; moving coil, moving iron, and moving magnet. Redlich [4] gives a summary and comparison of the types of linear motors and alternators from over twenty years of experience at Sunpower. The ASC uses a moving magnet type linear alternator with radial iron laminations and permanent magnets attached to the piston of the Stirling engine. The magnets pass back and forth through the alternator coil as the piston oscillates, creating a changing magnetic flux and inducing a voltage in the coil. Electrical power is output from terminals electrically connected to the alternator coil. The magnetic flux lines through the alternator are shown in Fig. 2, where the permanent magnet is displaced from the center.



The induced voltage, V_{emf} , from the alternator is in phase with the velocity of the piston; however, the coil has inductance that shifts the phase of the output voltage (V_{alt}). Inductance is defined in Equation (3). Further explanation of linear alternator operation, alternator inductance, or specifically the linear alternator of the ASC can be found in the Appendix B.

$$L = \frac{d\phi}{dI} = -\frac{V_{emf}}{\frac{dI}{dt}} \quad (3)$$

C. Statement of Problem

NASA's Glenn Research Center (GRC) is continuing development of free-piston Stirling convertor technology for space missions [5]. This includes testing of Stirling convertors [6] as well as computer modeling and simulation of Stirling systems [7]. Computer modeling can aid in the optimization of design and performance analysis of Stirling systems. Validated models can also help in the understanding of physical parameters that are impractical to test, or impossible to measure in Stirling devices and assist in system verification as well as space mission planning.

There have been many modeling and simulation efforts focused on the ASC. A review of these ASC modeling efforts is given in Chapter 2, along with a review of similar Stirling device and linear alternator modeling efforts. The primary goal of this thesis project is to develop a validated convertor model, Stirling engine and coupled linear alternator, using the Sage 1-D Stirling modeling software package. Two different linear alternator models are developed using Sage and are integrated with an existing

ASC Stirling engine model. The combined models are then tuned and validated against test data.

A secondary goal of the project is to develop a graphical user interface (GUI) to simplify the operation of the Sage model simulations and aid in analysis of simulation results. This will be accomplished using MATLAB to interface with Sage model files and perform post-simulation data processing. The final results of Sage simulations are output to a MATLAB GUI both in plain text as well as phasor diagrams to visualize ASC force components. Phasor analysis of the ASC is discussed in Chapter 2.

D. Thesis Statement

Two linear alternator models have been developed, integrated, and validated with a free-piston Stirling engine model of the ASC and can be used with a MATLAB GUI for analysis and planning of space power systems.

E. Limitations

The Sage model and MATLAB phasor analysis assumes the Stirling engine and linear alternator operation is purely sinusoidal. Sage is a 1-D modeling software and therefore unable to model inherently 3-D phenomena occurring in the ASC. Appendices A and B provide more detail to the limitations of the Sage models.

F. Definition of Terms

B_r	residual magnetic flux density (T)
K_i	alternator motor constant (N/A)
F	Force (N)
FringeMult	Sage fringe effect multiplier
I	current (A)
J_{Sat}	saturation magnetic polarization (T)
Jmult	Sage magnet strength multiplier
L_{alt}	alternator inductance (H)
N	number of turns
Q	net heat input (W)

R_{alt}	alternator resistance (Ω)
$R1, R2$	resistances (Ω)
$Sage_Q_{in}$	net heat input as calculated by Sage (W)
V_{emf}	electromotive force (EMF) voltage (V)
W_{net}	Power (W)
x	position (m)
μ_r	relative magnetic permeability (N/A ²)
ΔV	voltage (V)
Φ	magnetic flux (Wb)

G. Acronyms

ASC	Advanced Stirling Convertor
BOM	Beginning of mission
EM	Electromagnetic
EOM	End of mission
GRC	Glenn Research Center
GUI	Graphical user interface
HR	High reject (temperature)
LR	Low reject (temperature)
PM	Permanent magnet

Chapter II

Review of the Relevant Literature

This chapter will review literature covering the Sage Stirling modeling software, Stirling device modeling (including ASC modeling), linear alternator modeling, and phasor analysis of Stirling devices.

A. Sage 1-D Modeling Software for Stirling Devices

1. Sage Description and History

Sage [8] is a 1-D modeling software package for Stirling devices developed by Gedeon Associates. Sage contains a library of generic Stirling device components that can be placed and connected within the Sage GUI. Each component within Sages library can model particular aspects of a system and specific properties of the component are defined by the user [9]. Some components contain sub-components in a hierarchal fashion that further defines the system or sub-system being modeled. Model components are connected through interfaces that model the flow of energy between them (heat flow, volume flow, force, pressure, etc.). Figure 3 shows an example Sage model at the top level of the component hierarchy.

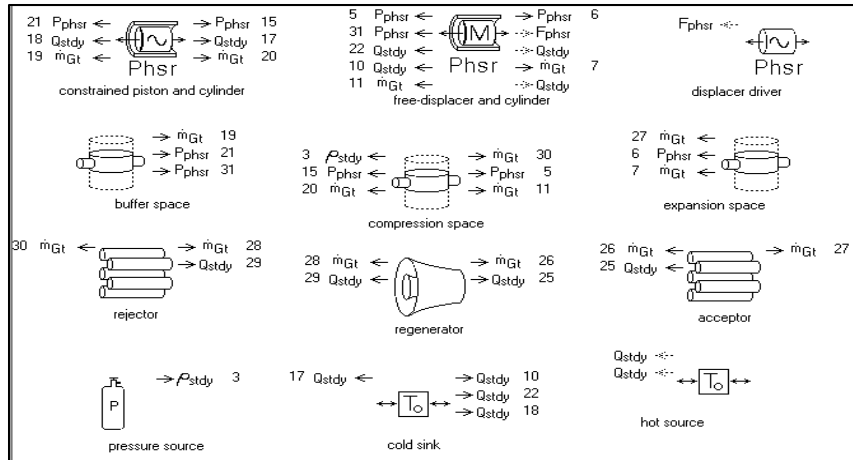


Figure 3. Sage GUI Components. Top level Sage components connected through energy flow interfaces.

Sage is the successor to the original GLIMPS/GLOP software developed by Gedeon Associates. GLIMPS was a 1-D code that modeled limited sections of a Stirling engine. GLOP was an optimization code used with GLIMPS to optimize design parameters of Stirling engines. Sage is based on these two codes and expanded to now model complete Stirling engines and models are created in a modular form [8]. Sage was first released in 1995 and is currently on its 9th version as of 2013. Each version has expanded Sages modeling library as well as improved its validity.

2. Sage Model Accuracy

Sage is the most widely used Stirling cycle modeling software, used by Stirling designers such as Sunpower, Inc. and INFINIA Corp. Demko and Penswick [10] provide a step-by-step reference to modeling with the Sage software. The paper showed results of modeling the 55W Technology Demonstration Converter (TDC) designed by INFINIA Corp. and compared simulation results to test data. Using this earlier version of Sage produced results that agreed with test data within 5% for predicted heat input, electric

power output, and net efficiency. Other parameters compared were within 20% of test data and investigation of model calibration factors were expected to produce better results. Qiu and Perterson [11] from the Stirling Technology Company (now INFINIA Corp.) also present Stirling modeling efforts using Sage. Un-calibrated models have an expected accuracy of 10-20% while models calibrated over a range of test data are expected to have accuracy within 5%.

Sage has also been compared to the more complex multi-dimensional computational fluid dynamic (CFD) model CFD-ACE+. Ebiana [12] presents results of heat transfer effects in a piston-cylinder setup with oscillating pressure and oscillating flow. Results of this work indicated that Sage is better at validating energy conservation than the CFD code and overall agrees well with CFD results, often within 5%. The CFD code has its own advantages though due to its ability to model inherently multi-dimensional characteristics such as turbulent fluid flow. Zhang and Ibrahim [13] also compared Sage against CFD-ACE+ using a scaled version of a Stirling Technology Company 55W Stirling Engine. Sage was compared to 2-D simulation results of the CFD code, although no test data was available for comparison.

3. Sage Electromagnetic (EM) Modeling

Sage version 9.1, released in January 2013, expanded the component library to include basic circuit and EM components. This enabled the modeling of EM devices such as electric actuators and generators, as well as devices with similar EM components. This addition also enables whole convertor (engine with alternator) modeling within Sage by allowing EM models to connect to mechanical components.

B. Stirling Engine and ASC Modeling

1. Stirling Cycle Modeling and Analysis Methods

Stirling cycle models are typically divided numerically into orders defined by Martini [14]. First order models are simplified “back of the envelope” based calculations that relate power output and efficiency of a Stirling engine to its temperature inputs, piston amplitude and frequency. This is often referred to as the Schmidt analysis and is used in preliminary design of Stirling devices. Second order models are often referred to as “modified Schmidt analysis” as they use the same basic equations but account for heat transfer losses and flow power losses.

Third order models use nodal analysis or control volumes to solve the governing 1-D physical equations [15]. Modeling codes such as GLIMPS and Sage are considered third order models. Other third order, 1-D, models include HFAST and the Stirling convertor System Dynamic Model (SDM) [16].

Multi-dimensional models such as CFD or finite element method (FEM) are considered fourth order models. These models can significantly expand analysis capabilities, however they are computationally intensive. Fourth order codes include CFD-ACE, Fluent, and Computer Aided Simulation of Turbulence (CAST) among others. A detailed review of Stirling modeling and analysis methods is given in [15].

2. Modeling of Stirling Devices with Sage

Sage has been used in modeling of many Stirling devices. Sunpower used Sage in the development of a 30 watt free-piston Stirling engine as well as the 80 watt ASC for NASA [17, 18]. In addition to smaller Stirling systems Sage has also been used to model larger kilo-watt Stirling engines. In [19], Sage is used to model a 12-kW free-piston

Stirling engine for the Fission Surface Power project at NASA GRC and was used in conjunction with MATLAB to produce performance maps to be used in a system model.

Sage is used in [20] to model an “off-design” Stirling engine, used to simulate changes in engine performance due to changes in operating conditions and design geometry caused by degradation of components. The model is also used to conduct sensitivity studies to determine how performance changes with varied parameters such as heat input, pressure, or appendix gap width. This paper highlights the capability of Sage in understanding Stirling engine performance and aiding in design.

The aforementioned SDM model was developed at GRC using the Simplorer™ software package. It was developed to be a whole convertor system model, capable of modeling non-linear dynamic behavior and startup transient behavior [21]. The SDM can also be set up with multiple convertor configurations and has been validated using test data from INFINIA’s 55W TDC. SDM is limited by a less sophisticated linear alternator model, less sophisticated thermodynamics, and extensive computation time.

C. Linear Alternator Modeling

1. Magnetic Circuit Analogy (Reluctance Network)

EM devices can be modeled using a magnetic circuit analogy. If the path of magnetic flux through a device is well defined then it can be understood as a magnetic circuit path and is analogous to an electric circuit [22]. The source of the magnetic flux is analogous to a voltage source and the elements along the magnetic path that have a magnetic reluctance are analogous to resistors (reluctance network). Figure 4 shows a magnetic circuit next to its analogous electric circuit.

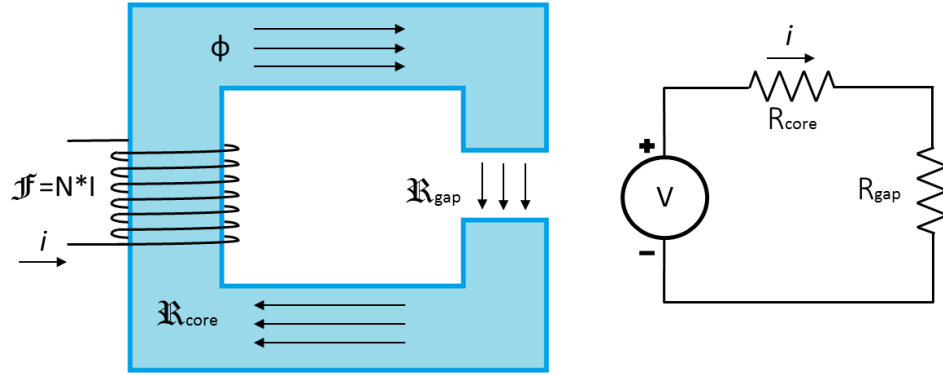


Figure 4. Magnetic Circuit Analogy. This figure shows a magnetic circuit and its equivalent electric circuit.

Sari [23] uses an FEM model to verify the design of an alternator and then develops a validated model based on the reluctance network method. This is combined with an analytical Stirling engine model to enable whole convertor modeling and system optimization. Similarly Cros [24] uses a reluctance network method to model a more complex high-power hydraulic synchronous generator and validates it against a more complex FEM model. More information on the magnetic circuit analogy can be found in Appendix B.

FEM software such as Maxwell is used for multidimensional modeling but can be computationally intensive. The Maxwell software has been used at GRC for evaluating linear alternator designs for Stirling convertors, including linear alternator of the 55W TDC. Cawthorne [25] also uses an FEM linear alternator model for a hybrid electric vehicle. The model is used to generate results of the position derivative of magnetic flux in the alternator at incremental positions. This was then used in a simplified circuit model to determine the induced voltage based on piston velocity.

D. Summary

Stirling devices are modeled using a variety of software and methods but few model a convertor from end-to-end. An end-to-end “whole convertor” model using a fourth order analysis is computationally intensive and difficult to validate. Using the latest version of the Sage software it is possible to model both the Stirling engine and linear alternator, enabling whole convertor modeling in a 1-D code that has proven reliable and is used by Stirling system designers. This thesis presents a whole convertor model built using the Sage model software package and validated using convertor test data from Sunpower and GRC.

Chapter III

Methodology

This chapter presents an overview of the methods used to model the ASC linear alternator using the Sage software and the use of phasor diagrams in Stirling system analysis. The linear alternator models created were integrated with a Sage ASC engine model provided by Sunpower and modified at GRC. Further details on linear alternator modeling can be found in Appendix B and details on phasor diagrams in Appendix A.

Both Sage alternator models were tuned using four key operating points of the ASC; beginning of mission (BOM) at low reject temperature (LR), BOM at high reject temperature (HR), end of mission (EOM) LR, and EOM HR. These operating points reflect the decay of the radioisotope fuel source, reducing heat input to the convertor and the range of rejection temperatures expected during a mission. ASC data at the BOM/EOM operating points is provided by Sunpower.

A. Sage Linear Alternator Modeling Using the Sage Transducer Component

1. Sage Transducer Component

The transducer model is the simplest method of modeling a linear alternator in Sage. The transducer component relates mechanical energy to electrical energy by a constant K_t (Eq. (6)). Voltage output of the transducer is found through the conservation of energy as shown in Equation (7).

$$F = K_t * I \quad (6)$$

$$F dx/dt = \Delta VI \quad (7)$$

The component has both force and current interfaces to link mechanical and electrical systems (Fig. 5).

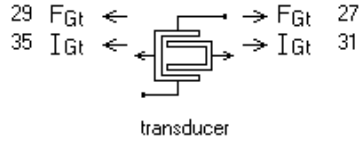


Figure 5. Sage Transducer Component. The transducer component is used to model the conversion of mechanical energy to electrical energy.

2. Sage Transducer Model Circuit

In addition to the transducer component, a resistor and inductor component are used to account for the resistance and inductance of the alternator coil. Figure (6) shows a Sage transducer alternator model connected to the convertor controlling circuit. The outlined components make up the alternator model.

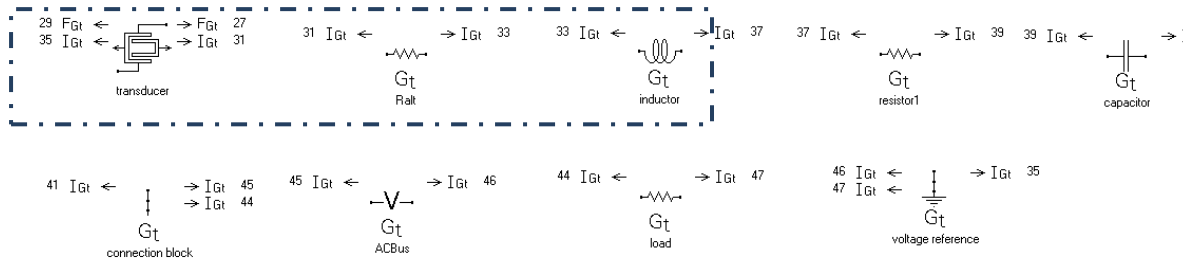


Figure 6. Sage Transducer Alternator Model. This model shows the three key alternator components (outlined) connected to the convertor controlling circuit.

3. Sage transducer Model Tuning

The transducer component does not model other losses typical of magnetic circuits such as eddy-currents, hysteresis loss, and flux leakage. These losses are added to the resistive

loss of the alternator coil and the model was tuned to find the correct resistive value, R_{loss} . As discussed in Appendix B, the resistive term R_{loss} and the motor constant K_i are temperature dependent and the values were tuned across multiple data points.

B. Sage Linear Alternator Model Using EM Components

The EM alternator model is the more complex method of linear alternator modeling in Sage. This method assumes a generic shape of the linear alternator (Fig. 7) and models the physical characteristics using EM model components. The geometry of the components is user defined while parameters such as coil resistance and inductance are outputs calculated from the geometry of the component. Figure (8) shows the structure of the Sage model components. The Sage EM model solution is based on the magnetic circuit analogy as described in Chapter 2, and further described in Appendix B.

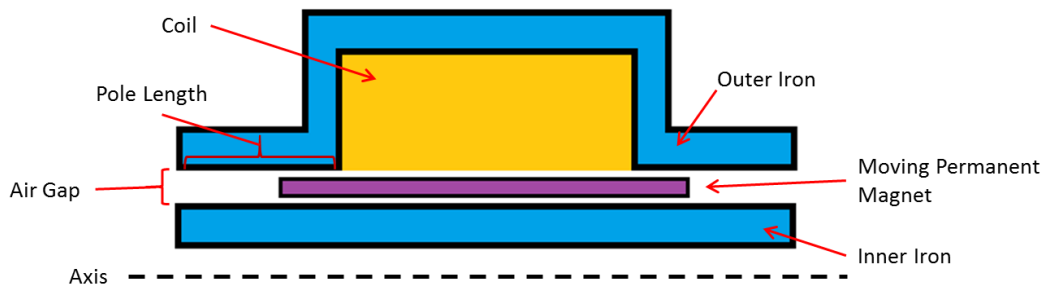


Figure 7. Generic Linear Alternator Diagram. This diagram shows the generic shape the Sage alternator model assumes.

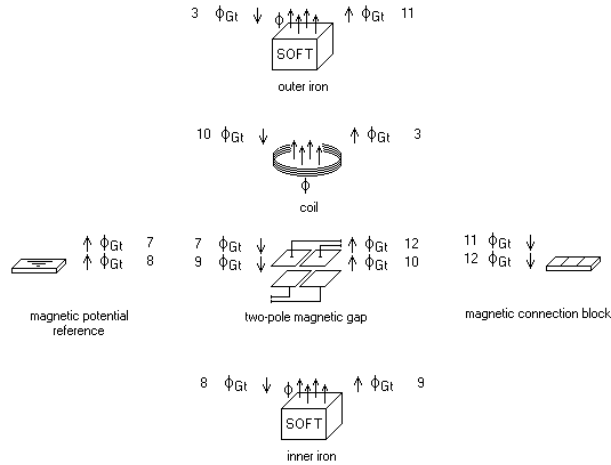


Figure 8. Sage EM Alternator Model Structure. The figure shows the high-level components that create the EM alternator model structure.

1. Sage EM Alternator Model Tuning

The Sage EM components have two built in tuning parameters; J_{mult} and $FringeMult$. These parameters tune the magnet strength and magnetic fringe effect, respectively. The Sage EM components have built in temperature dependence for the alternator coil, permanent magnet, and iron cores, unlike the transducer component which does not have temperature dependence. For this reason the EM model was not tuned across the four BOM/EOM operating points. Instead, the J_{mult} and $FringeMult$ parameters were tuned to match the measured inductance of the ASC alternator and alternator performance at the BOM-LR operating point. Further details regarding the Sage EM alternator model development is in Appendix B.

C. Phasor Diagram Analysis of Stirling Systems

1. Phasor Diagrams

The forces operating in the ASC are sufficiently sinusoidal to be analyzed using phasor diagrams. ASC components oscillate at the same frequency but with varied phase

as shown by the force diagram in Fig. 9. These forces can instead be represented by phasors and aligned (Fig. 10) to visually verify Newton's second law, $F=ma$. This provides a more intuitive method of analyzing ASC forces and also can be applied to alternator voltages. More information on phasor diagrams is presented in Appendix A.

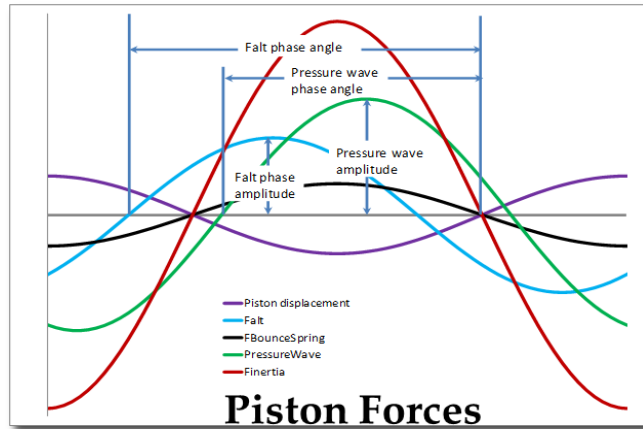


Figure 9. Sinusoidal Piston Forces Diagram. This figure shows the phase difference of forces acting on the ASC piston.

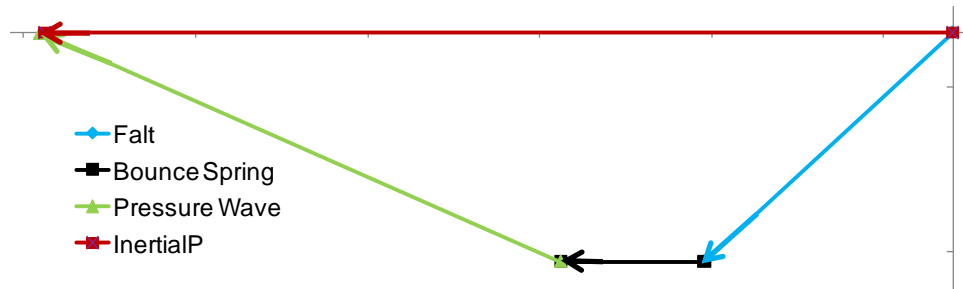


Figure 10. Phasor Diagram of Piston Forces. This figure shows the same piston forces from Fig. 9 represented in phasor form and aligned to show $F=ma$.

2. Sage/MATLAB Interface

Sage does not provide the ability to generate phasor diagrams from the model results; however, it does allow access to the model through a C++ compiler and a Sage

dynamic link library (dll) file. This enables a program such as MATLAB to be used to operate the Sage model, save model output results, and then conduct post-processing operations on the data. Figure 11 depicts the interaction between MATLAB and Sage.

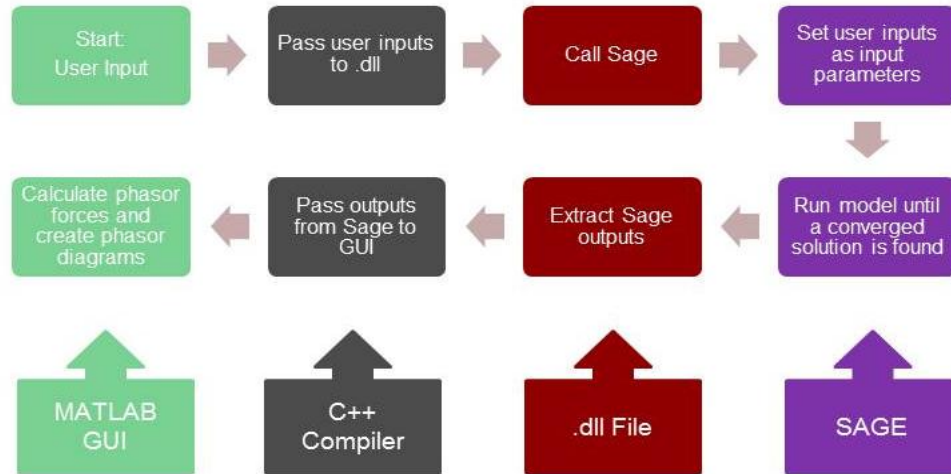


Figure 11. Diagram of MATLAB and Sage Interaction. This diagram shows the process in which MATLAB can access and operate a Sage model file.

3. MATLAB GUI

To operate the Sage model and automate the simulation and phasor diagram process a MATLAB GUI was developed. The GUI allows model inputs to be quickly changed and simulation results to be presented in a more intuitive manner. It also allows phasor results to be held across multiple simulations to observe how varied parameters change performance. Figure 12 shows an example MATLAB GUI with phasor diagrams from a Sage model. More information on the Sage/MATLAB GUI is presented in Appendix A.

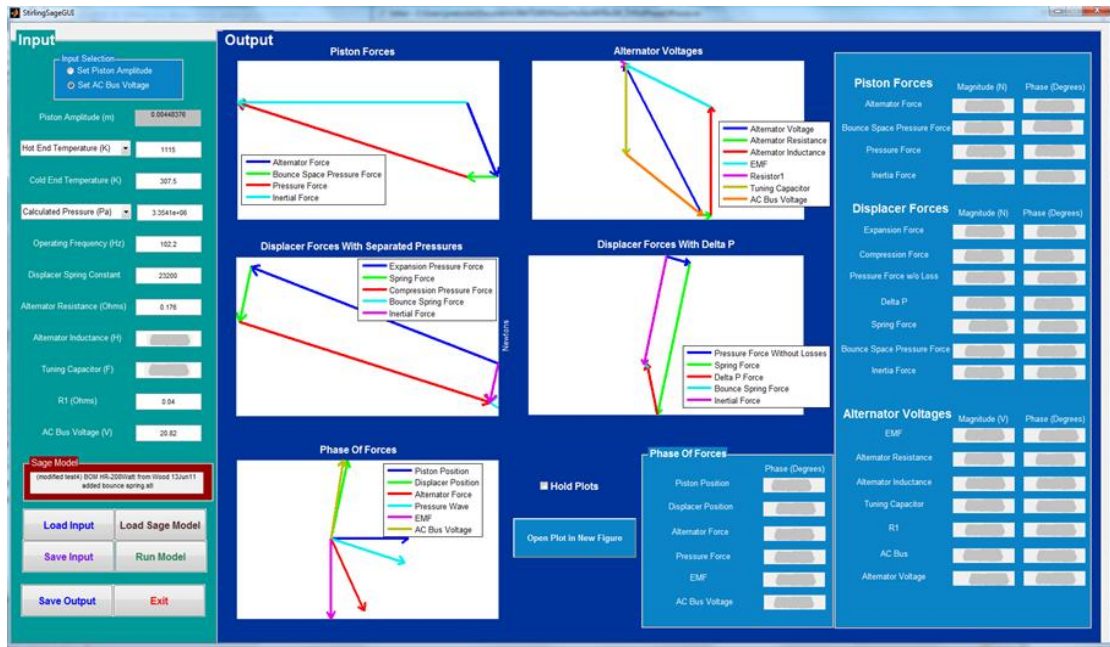


Figure 12. MATLAB GUI with Phasor Diagrams. This figure shows a MATLAB GUI with phasor diagrams from Sage model output.

Chapter IV

Results

This chapter presents the results of the combined ASC engine and linear alternator models. The models were tuned using data from Sunpower during the manufacturing process and then tested against Sunpower data at the EOM/BOM operating conditions as well as performance map data gathered at GRC. Further detail on results from the Sage models is found in Appendix B.

A. Sage ASC with Transducer Alternator Results

1. Results at EOM/BOM Operating Conditions

The transducer model was tuned across all four EOM/BOM points; consequently results were expected to agree well with EOM/BOM test data from Sunpower. Table 1 shows the percent difference between the model and test data the four operating points.

Table 1. Transducer Model Results vs. Sunpower Data. These results show the percent difference between the model output and data from Sunpower at the four operating conditions.

Test Parameters Sage Transducer Alternator Model	BOM-LR	BOM-HR	EOM-LR	EOM-HR
Net-heat input, Q (W)	2.29%	-2.14%	5.37%	-2.36%
Piston Amplitude (mm)	0.00%	0.00%	0.00%	0.00%
Displacer Amplitude (mm)	0.73%	1.30%	0.82%	0.85%
Displacer to Piston Phase (degree)	1.01%	0.11%	2.03%	0.38%
Piston to Current Phase (degree)	-0.11%	2.30%	-1.51%	1.92%
Terminal power (W)	-0.27%	0.38%	0.64%	-0.46%
Power factor	0.21%	-0.43%	0.25%	0.30%
Voltage rms (V)	-2.64%	-2.43%	-1.18%	-2.78%
Current rms (A)	2.08%	2.38%	2.01%	2.37%
Efficiency (%)	-2.51%	2.58%	-4.49%	1.95%

2. Results from GRC Performance Map

The model was tested against performance map data gathered at GRC for which the model was not tuned. Figure 13 shows convertor efficiency data at multiple operating

points as a function of rejection temperature. Piston amplitude also varies along these points. Acceptor temperature, rejector temperature and piston amplitude were matched in the Sage model. The numbers next to each data point indicate the net heat input, Q (W), input to the convertor.

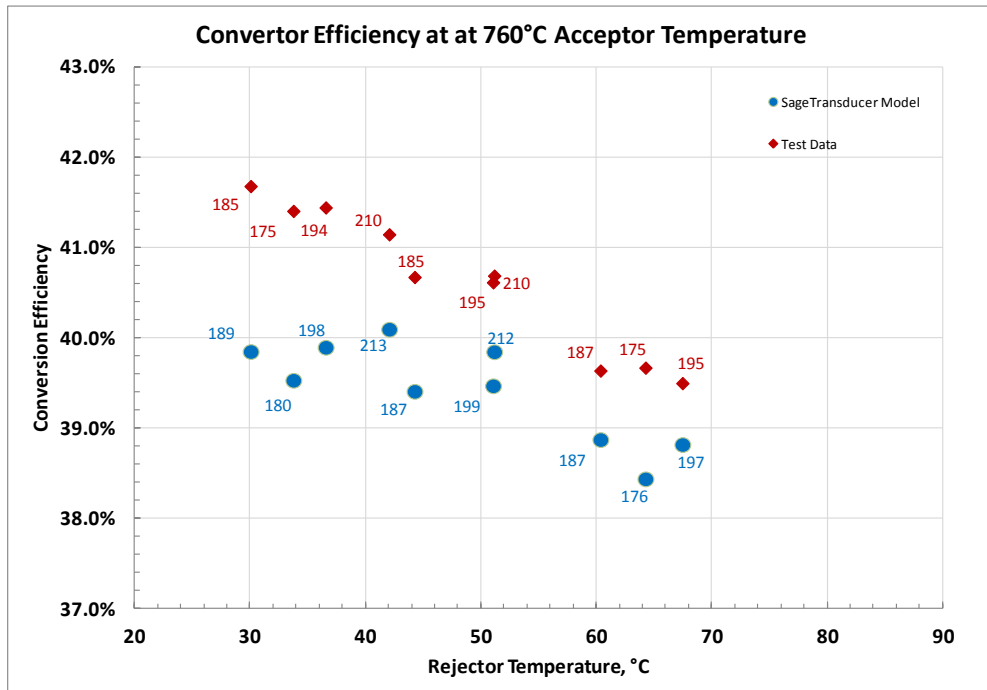


Figure 13. Transducer Model Performance Map Comparison of Convertor Efficiency. This figure shows model results and test data from at performance map test points.

Figure 14 shows convertor power output data from the GRC performance map along with Sage model results. The largest difference between model and data results is approximately 3W.

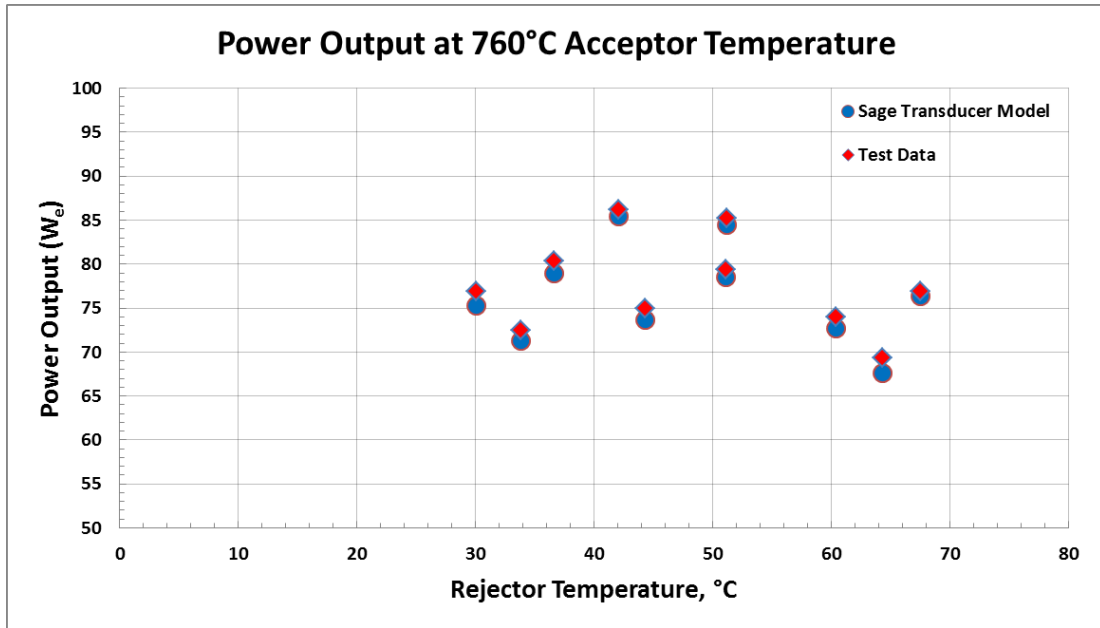


Figure 14. Transducer Model Performance Map Comparison of Power Output. This figure compares the power output from performance map data gathered at GRC to Sage model output at the same operating conditions.

B. Sage ASC with EM Alternator Model Results

1. Results at EOM/BOM Operating Conditions

The EM model was tuned only at the BOM-LR point as the model was designed to account for changes in temperature, unlike the transducer model. Table 2 shows the results comparing the model to test data at the BOM/EOM operating conditions. The results agree well but are not as consistent across the operating points. The LR points are similar but the HR points have larger error. This suggests that the model does not fully account for changes in performance due to temperature.

Table 2. EM Model Results vs. Sunpower Data. These results show the percent difference between the model output and data from Sunpower at the four operating conditions.

Test Parameters Sage EM Alternator Model	BOM-LR	BOM-HR	EOM-LR	EOM-HR
Net-heat input, Q (W)	-1.03%	-5.07%	1.92%	-5.45%
Piston Amplitude (mm)	0.00%	0.05%	-0.05%	-0.05%
Displacer Amplitude (mm)	-1.40%	-0.92%	-1.36%	-1.56%
Displacer to Piston Phase (degree)	-0.89%	-1.26%	-0.02%	-0.94%
Piston to Current Phase (degree)	0.44%	1.87%	-0.80%	1.92%
Terminal power (W)	0.44%	-3.96%	3.92%	-4.72%
Power factor	0.46%	1.45%	-0.63%	3.43%
Voltage rms (V)	-0.85%	-5.02%	2.57%	-5.32%
Current rms (A)	0.89%	-1.75%	1.70%	-2.37%
Efficiency (%)	1.48%	1.16%	1.96%	0.77%

2. Results from GRC Performance Map

The EM model was tested against performance map data gathered at GRC. Figure 15 shows convertor efficiency data at multiple operating points as a function of rejection temperature. Acceptor temperature, rejector temperature and piston amplitude were matched in the Sage model. The numbers next to each data point indicate the net heat input, Q (W), input to the convertor.

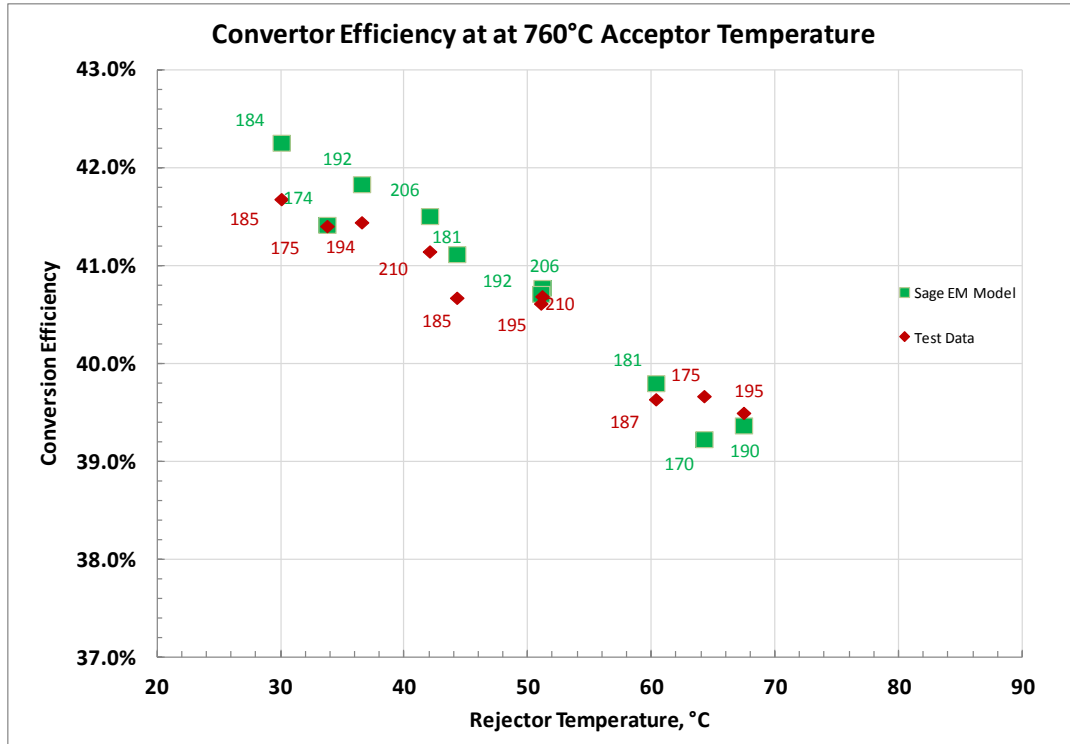


Figure 15. EM Model Performance Map Comparison of Converter Efficiency. This figure shows model results and test data from at performance map test points.

Figure 16 shows convertor power output data from the GRC performance map along with Sage model results. The difference between model results and test data increases with increasing rejector temperature to maximum difference of 3W.

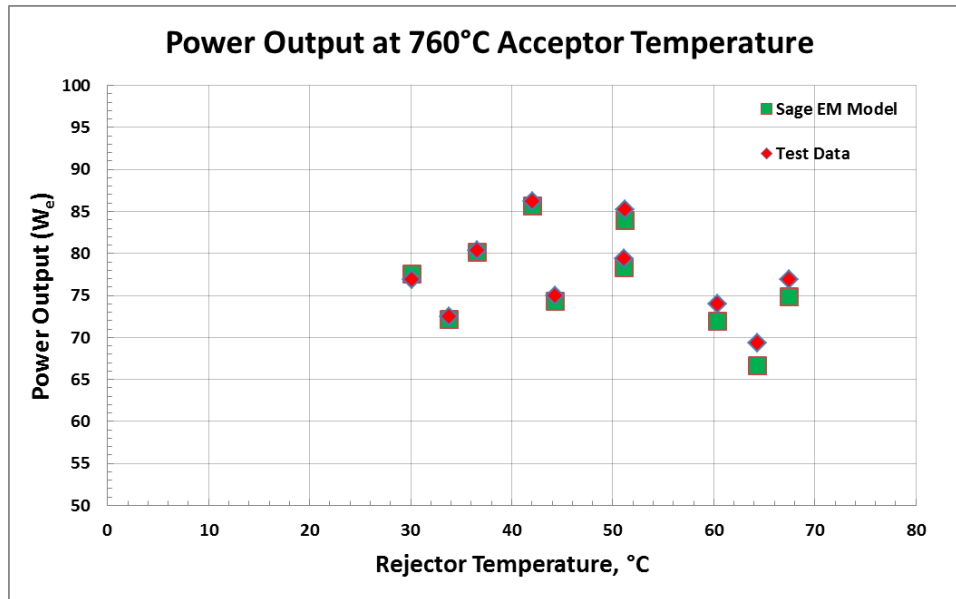


Figure 16. EM Model Performance Map Comparison of Power Output. This figure compares the power output from performance map data gathered at GRC to Sage model output at the same operating conditions.

C. Sage Alternator Comparison

Figure 17 and 18 show a comparison between the transducer alternator model and the EM alternator model against Sunpower BOM/EOM test data. It also shows the default (un-tuned) model performance. Further detail on model results is in Appendix B.

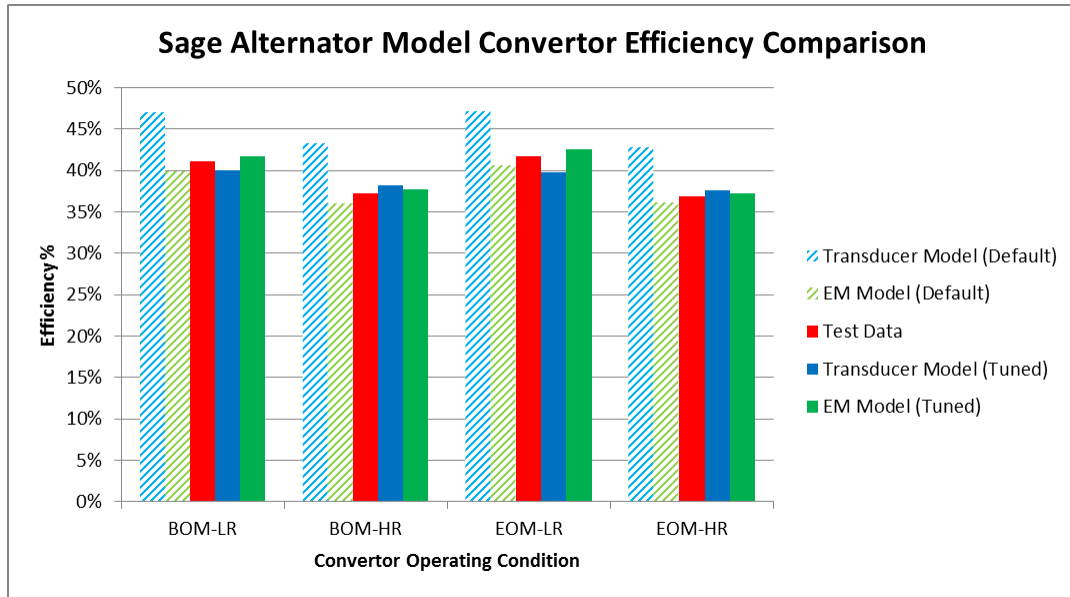


Figure 17. Alternator Model Comparison of Efficiency Results. This figure shows the default and tuned transducer and EM model results compared to test data.

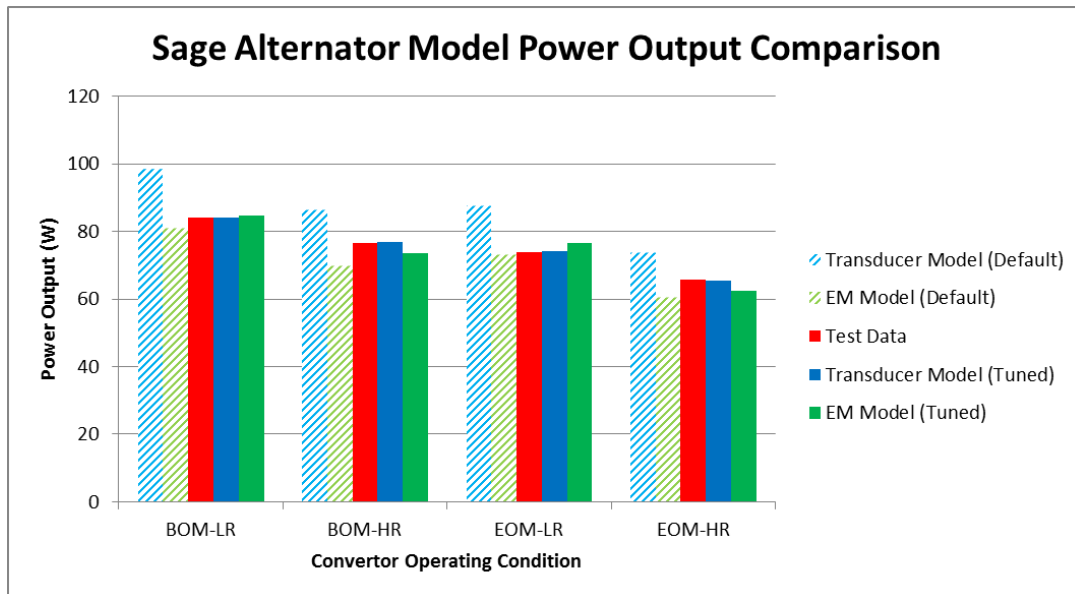


Figure 18. Alternator Model Comparison of Power Output Results. This figure shows the default and tuned transducer and EM model results compared to test data.

Chapter V

Discussion, Conclusions, and Recommendations

Discussion

Two linear alternator models were developed using the Sage software and integrated with a free-piston Stirling engine model of the ASC. The models were tuned to test data gathered at Sunpower, Inc. during manufacturing and verification. The tuned models were then validated against performance map data of the ASC gathered at GRC. The whole convertor models developed in Sage enables ASC simulations to be conducted using a single model that is not as computationally intensive as multidimensional CFD models.

In addition a MATLAB GUI has been created to operate the Sage models and automate simulation and phasor diagram analysis. This enables greater understanding of ASC operation by using a visual interpretation of model results as well as allows users without ASC modeling experience to operate Sage models.

Conclusions

Both of the validated integrated ASC models agree with data within 7% or less. The transducer model is more consistent across a range of operating points, but must be tuned using multiple data sets due to its simplified relationship between piston motion and electric power generated. The EM model is created entirely from first principles. As an un-validated model it is useful as a parameter sensitivity design tool. After tuning and validation the model results matched experimental data within 7%.

Recommendations

The EM alternator model agrees well with data but it is not as consistent as the validated transducer model. The model was tuned at a low rejection temperature operating point and model error increases with increasing temperature, suggesting the model does not properly account for changes in performance at higher temperatures. This could be due to inaccurate permanent magnet or iron core material data which assumes magnet strength and magnetic saturation (respectively) decrease linearly to zero at the Curie temperature. These phenomena could be investigated to provide more consistent results when using the EM alternator model.

References

- [1] Schreiber, Jeffrey G., "Assessment of the Free-Piston Stirling Convertor as a Long Life Power Convertor for Space," in Proceedings of the 35th Intersociety Energy Conversion Engineering Conference (IECEC) 2000. Institute of Electrical and Electronics Engineers, Las Vegas, Nevada, 24-28 July 2000.
- [2] Thieme, Lanny G., and Jeffrey G. Schreiber. "NASA GRC technology development project for a Stirling radioisotope power system." In *Energy Conversion Engineering Conference and Exhibit, 2000.(IECEC) 35th Intersociety*, vol. 1, pp. 249-258. IEEE, 2000.
- [3] Richardson, R. and Chan, J., "Advanced Stirling Radioisotope Generator," Proceedings of NASA Science Technology Conference (NSTC 2007)
- [4] Redlich, Robert, "A Summary of Twenty Years Experience with Linear Motors and Alternators," published by Sunpower, Inc., 1995.
- [5] Thieme, Lanny G., Jeffrey G. Schreiber, and Lee S. Mason. *Stirling technology development at NASA GRC*. National Aeronautics and Space Administration, Glenn Research Center, 2001.
- [6] Williams, Zachary D., and Oriti, Salvatore M. "Advanced Stirling Convertor (ASC-E2) Characterization Testing," in *Proceedings of the Tenth International Energy Conversion Engineering Conference (IECEC 2012)* American Institute for Aeronautics and Astronautics, 2012.
- [7] Tew, R.C., Cairelli, J.E., Ibrahim, M.B., Simon, T.W., Gedeon, D., *Overview of NASA Multi-Dimensional Stirling Convertor Code Development and Validation Effort*. National Aeronautics and Space Administration, Glenn Research Center, 2002.
- [8] Gedeon, David. "Sage: Object Oriented Software for Stirling Machine Design," AIAA Paper 94-4106-CP. 1994.
- [9] Gedeon, David. "Sage User's Guide, Ninth Edition," Gedeon Associates, 2013.
- [10] Demko, Rikako and Penswick, L. Barry., "Sage Simulation Model for Technology Demonstration Convertor by a Step-by-Step Approach," in *Proceedings of the Third International Energy Conversion Engineering Conference (IECEC 2005)* American Institute for Aeronautics and Astronautics, 2005.
- [11] Qiu, Songgang, and Peterson, Allen A., "Linear Dynamic Modeling and Numerical Simulation of an STC Stirling Convertor," in *Proceedings of the First*

- International Energy Conversion Engineering Conference (IECEC 2003)*, American Institute for Aeronautics and Astronautics, 2003.
- [12] Ebiana, A. B., Savadekar, R.T., Vallury, A. “2nd Law Analysis of Sage and CFD-ACE+ Models of MIT Gas Spring and “Two-Space” Test Rigs,” in *Proceedings of the Second International Energy Conversion Engineering Conference (IECEC 2004)* American Institute for Aeronautics and Astronautics, 2004.
- [13] Zhang, Zhiguo and Ibrahim, Mounir. “Development of CFD model for Stirling Engine and its Components,” in *Proceedings of the Second International Energy Conversion Engineering Conference (IECEC 2004)* American Institute for Aeronautics and Astronautics, 2004.
- [14] Martini, William R., *Stirling Engine Design Manual*. National Aeronautics and Space Administration, Lewis Research Center, 1983.
- [15] Dyson, Rodger W., Scott D. Wilson, and Roy C. Tew. "Review of Computational Stirling Analysis Methods," in *Proceedings of the Second International Energy Conversion Engineering Conference (IECEC 2004)* American Institute for Aeronautics and Astronautics, 2004.
- [16] Dyson, Rodger W., Wilson, Scott D., Tew, Roy C., and Demko, R. "On the Need for Multidimensional Stirling Simulations," in *Proceedings of the Third International Energy Conversion Engineering Conference (IECEC 2005)* American Institute for Aeronautics and Astronautics, 2005.
- [17] Wood, J. Gary, and Neill Lane. "Advanced small free-piston stirling convertors for space power applications." In *AIP Conference Proceedings*, pp. 440-444. IOP INSTITUTE OF PHYSICS PUBLISHING LTD, 2004.
- [18] Wood, J. Gary, Cliff Carroll, and L. B. Penswick. "Advanced 80 We Stirling Convertor Development Progress." In *Space Technology and Applications International Forum (STAIF 2005)*, Albuquerque, NM. 2005.
- [19] Briggs, Maxwell H., “Implementation of a Sage-Based Stirling Model Into a System-Level Numerical Model of the Fission Power System Technology Demonstration Unit,” in *Proceedings of Nuclear and Emerging Technologies for Space*, (NETS-2011), Albuquerque, New Mexico, 2011.
- [20] Ebiana, A.B., Tew, R.C., and Regan, T.F., “An Off-Design Sage Thermodynamic Model of a Scaled Stirling Engine”, in *Proceedings of the First International Energy Conversion Engineering Conference (IECEC 2003)* American Institute for Aeronautics and Astronautics, 2003.
- [21] Lewandowski, E.J., and Regan, T.F., “Overview of the GRC Stirling Convertor System Dynamic Model,” in *Proceedings of the Second International Energy*

Conversion Engineering Conference (IECEC 2004), American Institute of Aeronautics and Astronautics, 2004.

- [22] Reitz, J.R., Milford, F.J, and Christy, R.W., *Foundations of Electromagnetic Theory*, 3rd ed., Addison-Wesley Publishing Company, Inc., Reading, MA, 1980, Chaps. 9-12.
- [23] Sari, Ali, Christophe Espanet, Francis Lanzetta, Didier Chamagne, Didier Marquet, and Philippe Nika. "Design and performance prediction of miniaturized Stirling power generators." In *Telecommunications Energy Conference, 2008. INTELEC 2008. IEEE 30th International*, pp. 1-7. IEEE, 2008.
- [24] Cros, J., Taghizadeh, M., Figueroa, J.R., Radaorozandry, L., Viarouge, P. "Simplified design model for fast analysis of large synchronous generators with magnetic saturation," in *Proceedings of International Electric Machines and Drives Conference, 2009. International Electrical and Electronics Engineers*, Miami, Florida, 3-6 May 2009.
- [25] Cawthorne, William R., Parviz Famouri, Jingdong Chen, Nigel N. Clark, Thomas I. McDaniel, Richard J. Atkinson, Subhash Nandkumar, Christopher M. Atkinson, and Sorin Petreanu. "Development of a linear alternator-engine for hybrid electric vehicle applications." *Vehicular Technology, IEEE Transactions on* 48, no. 6 (1999): 1797-1802.

Appendix A

Appendix A contains the first conference paper titled, “Development and Integration of an Advanced Stirling Convertor Linear Alternator Model for a Tool Simulating Convertor Performance and Creating Phasor Diagrams.” This paper is authored by Jonathan Metscher and Edward Lewandowski and is published in the Proceedings of the Eleventh International Energy Conversion Engineering Conference (IECEC 2013), American Institute for Aeronautics and Astronautics, in San Jose, CA.

Development and Integration of an Advanced Stirling Converter Linear Alternator Model for a Tool Simulating Converter Performance and Creating Phasor Diagrams

Jonathan F. Metscher¹ and Edward J. Lewandowski²
NASA Glenn Research Center, Cleveland, OH 44135

A simple model of the Advanced Stirling Converter's (ASC) linear alternator and an AC bus controller has been developed and combined with a previously developed thermodynamic model of the converter for a more complete simulation and analysis of the system performance. The model was developed using Sage, a 1-D thermodynamic modeling program that now includes electro-magnetic components. The converter, consisting of a free-piston Stirling engine combined with a linear alternator, has sufficiently sinusoidal steady-state behavior to allow for phasor analysis of the forces and voltages acting in the system. A MATLAB graphical user interface (GUI) has been developed to interface with the Sage software for simplified use of the ASC model, calculation of forces, and automated creation of phasor diagrams. The GUI allows the user to vary converter parameters while fixing different input or output parameters and observe the effect on the phasor diagrams or system performance. The new ASC model and GUI help create a better understanding of the relationship between the electrical component voltages and mechanical forces. This allows better insight into the overall converter dynamics and performance.

Nomenclature

C_f	=	alternator motor constant (N·s/m)
F	=	Force (N)
FF	=	sinusoidally varying forcing function (N)
I	=	current (A)
L_{alt}	=	alternator inductance (H)
N	=	number of turns
Q_{in_net}	=	net heat input (W)
t	=	time (s)
R_{alt}	=	alternator resistance (Ω)
$R1, R2$	=	resistances (Ω)
$Sage_Q_{in}$	=	net heat input as calculated by Sage (W)
V_{emf}	=	electromotive force (EMF) voltage (V)
W_{net}	=	Power (W)
x	=	position (m)
ΔV	=	voltage (V)
Φ	=	magnetic flux (Wb)

¹ Co-op Student, Thermal Energy Conversion Branch, 21000 Brookpark Rd.

² Deputy Lead, ASRG Power System, Thermal Energy Conversion Branch, 21000 Brookpark Rd., AIAA Senior Member.

I. Introduction

THE Advanced Stirling Radioisotope Generator (ASRG) is a radioisotope power system being developed for future NASA deep space missions, where solar power is not feasible. Current radioisotope thermoelectric generators (RTGs) provide reliable electric power for long duration space missions; however they have low conversion efficiency (around 5-7%). The heat source used for the RTGs is the General Purpose Heat Source (GPHS) which generates heat by the radioactive decay of Plutonium-238, a limited resource that is only just starting to be produced again in the U.S. The Multi-Mission RTG (MMRTG) powering the Mars Science Laboratory Rover Curiosity uses eight GPHS modules. The ASRG is a higher-efficiency system, requiring two GPHS modules. The ASRG achieves this by using highly efficient Stirling engines¹.

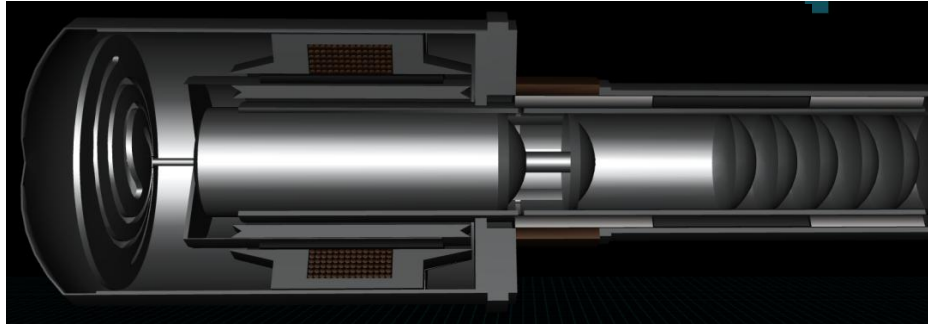


Figure 1. Cutaway of the Advanced Stirling Converter (ASC).

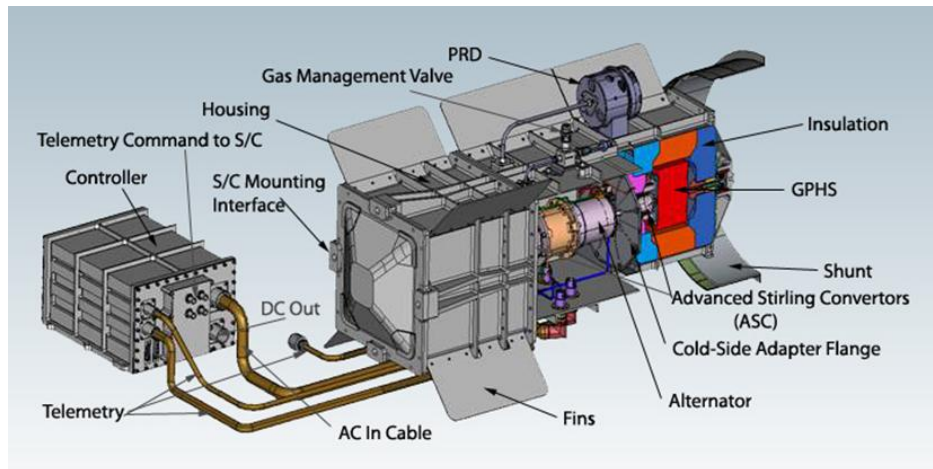


Figure 2. ASRG Diagram

The Advanced Stirling Converter (ASC), developed by Sunpower, Inc., is a free-piston Stirling engine coupled with a linear alternator (Fig. 1). The converter consists of a helium filled, hermetically sealed, pressure vessel containing a displacer, piston, and the linear alternator. Heat is input to the system from a GPHS to heat the working fluid (helium). The piston is initially put into motion by the alternator as an AC voltage is applied. The working fluid is shuttled between the compression space and expansion space through heat exchangers and regenerator for increased efficiency. The oscillating pressure of the working fluid imparts a force on the displacer. A spring located in the bounce space provides a restoring force for the displacer whereas the bounce space pressure acts as a gas spring providing a restoring force for the piston. Magnets are attached to the piston allowing piston motion to be converted to electric power by the linear alternator. The linear alternator provides a damping force on the piston as well as a spring-like restoring force. To minimize vibrations in the ASRG, two ASCs are mounted opposite of each other and their piston strokes are controlled electrically by adjusting the AC bus voltage and phase of alternator (Fig. 2). The ASRG requires only two GPHS modules (one per ASC), a factor of 4 reduction in Plutonium-238 usage relative to an MMRTG, while providing comparable electric power output².

A. Phasor Analysis

To accomplish control of the ASC along with maximizing efficiency requires a better understanding of the interaction of components and relationship of forces acting on those components. Insight into convertor dynamics can be gained by plotting the forces acting on components. A time dependent plot of the forces acting on the piston is shown in Fig. 3.

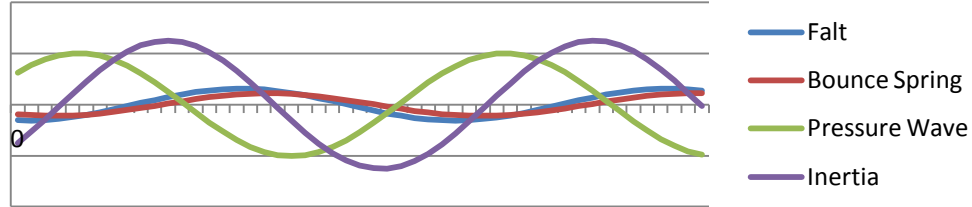


Figure 3. Time dependent plot of piston forces.

The components of a Stirling engine oscillate at the same frequency but vary in phase³. The forces are also sufficiently sinusoidal to be represented as phasors. This is a more useful method for plotting the time varying forces as it more clearly shows how forces change in response to a change in system parameters⁴. It is also a more intuitive method as all the force phasors added together should be equivalent to the inertia phasor, verifying $F = ma$. Figure 4 is a typical phasor diagram of forces acting on the piston.

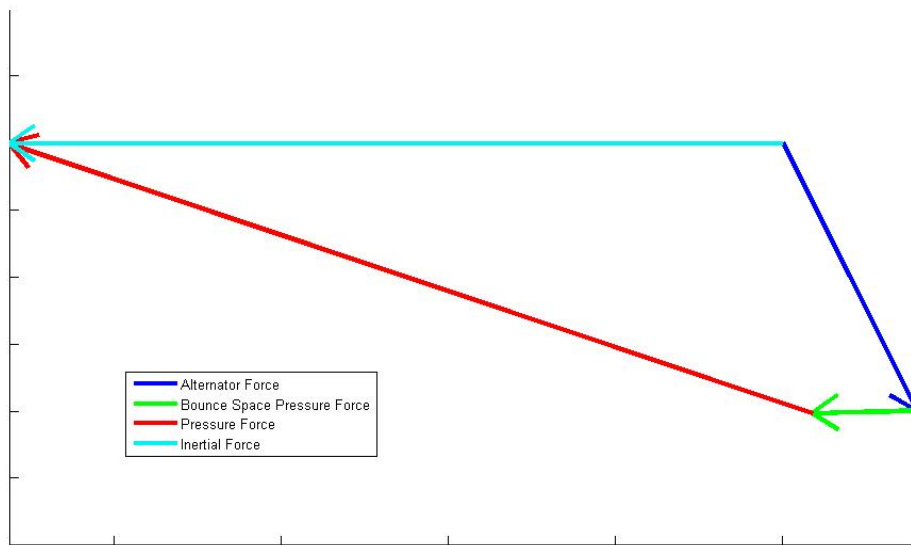


Figure 4. Phasor diagram of piston forces.

B. Sage Software

The Sage software package, developed by Gedeon Associates, is a 1-D thermodynamic modeling software for Stirling machines. It contains a library of generic model components which can be interconnected through the graphical user interface to create a model. The user can set both model geometry as well as initial model parameters. Sage can then use an iterative solver to find a converging solution to the system that balances energy flows and temperatures at interfaces, provided that the model is physically sound and input values are reasonable starting values. Sage also supports user-defined variables, and typically independent Sage model parameters can also be recast as dependent variables and defined through algebraic expressions. Design optimization is also supported by defining constraints and setting optimized variables, making Sage a powerful software tool for the development and analysis of Stirling engines⁵.

To build a model, Sage model components are selected and placed into the edit space. Many components allow for sub-components to be placed within the main (or parent) components. Some component interfaces are automatically generated while others may be added individually. These interfaces are the physical inputs and outputs of components such as force, pressure, heat flow, mass flow, and so on. The interfaces are connected from one component to another as can be seen in Fig. 5 below. The Sage model does not give a physical sense of the geometry of the system, however it does give a sense of the physical interactions between components.

It should also be noted that there are two general types of Sage components: time-ring and phasor. Phasor components assume purely sinusoidal motion without harmonics and input/output is given by a magnitude and an angle. "Time-ring" components do not assume purely sinusoidal motion and are solved along a time-grid. Input/output for time-ring components are given as a Fourier series. Time-ring and phasor components cannot be connected unless a motion filter is applied. The motion filter forces the time-ring components solution grid to have sinusoidal characteristics. This can cause some loss of physical properties if the system has significant non-linear properties. The ASC is modeled with phasor components as the steady-state motion is very nearly sinusoidal (Fig. 5).

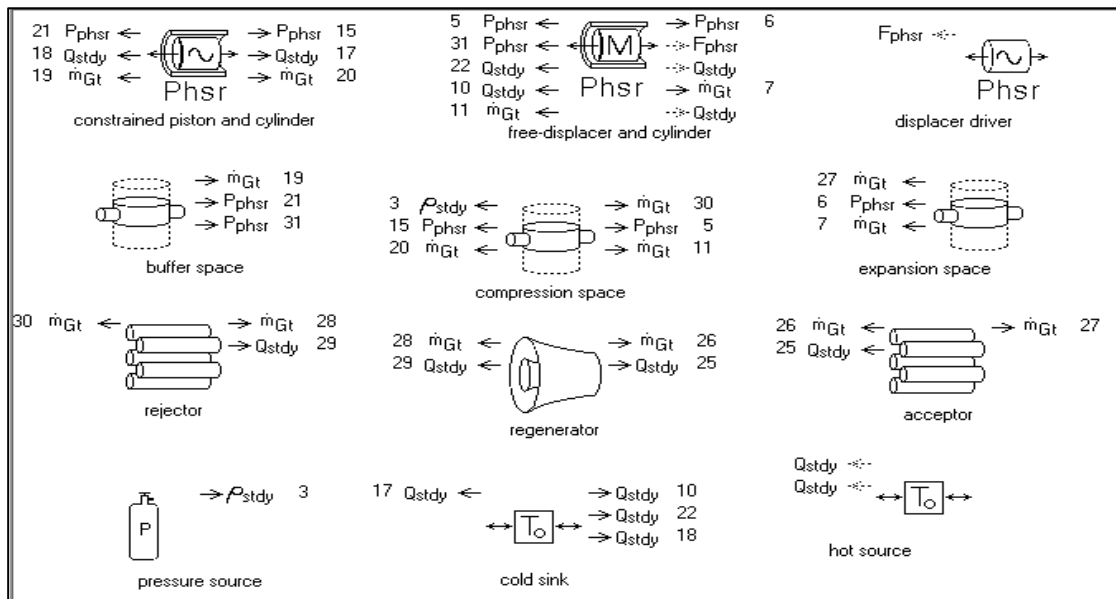


Figure 5. Sage Stirling engine model.

C. MATLAB Graphical User Interface

Sage is also available as a dynamic link library (dll) file which allows access to Sage models from another program running in the Windows operating system using a C++ compiler. MATLAB is such a program that can use a C++ compiler to run the Sage dll. Model parameters can be accessed and changed from the dll file, and outputs can be calculated and exported. When the simulation is executed, MATLAB passes the input parameters to the corresponding model input in the dll file. The dll file calls the Sage solver to update the input parameters and run the model to find a solution. The outputs are then passed back to the dll file and are available to the MATLAB GUI. Figure 6 shows the interaction between MATLAB and Sage.

Previously, a MATLAB GUI (Fig. 7) was developed to interface with the Sage dll to vary input parameters and plot calculated outputs in phasor diagram form⁶. The user selects the Sage model from a library of models and defines the input parameters from the MATLAB GUI. The outputs from the Sage model are used to determine the forces acting on the components and plot phasor diagrams. Plots can be held from run to run and overlaid to show how forces vary as input parameters are changed. The displacer and piston phasor diagrams are drawn with the piston phase along the x-axis.

The Sage model of the ASC and corresponding MATLAB phasor output shown in Fig. 7 does not include the linear alternator dynamics. This model also requires piston amplitude to be set, whereas a more realistic model would allow piston amplitude to change as other operating parameters were varied. Another limitation concerns the heat input parameter which is input as the hot-end temperature. To model an ASC powered by a GPHS, the user should be able to be set the heat input in watts from the heat source and have the tool calculate the temperature at the hot end.

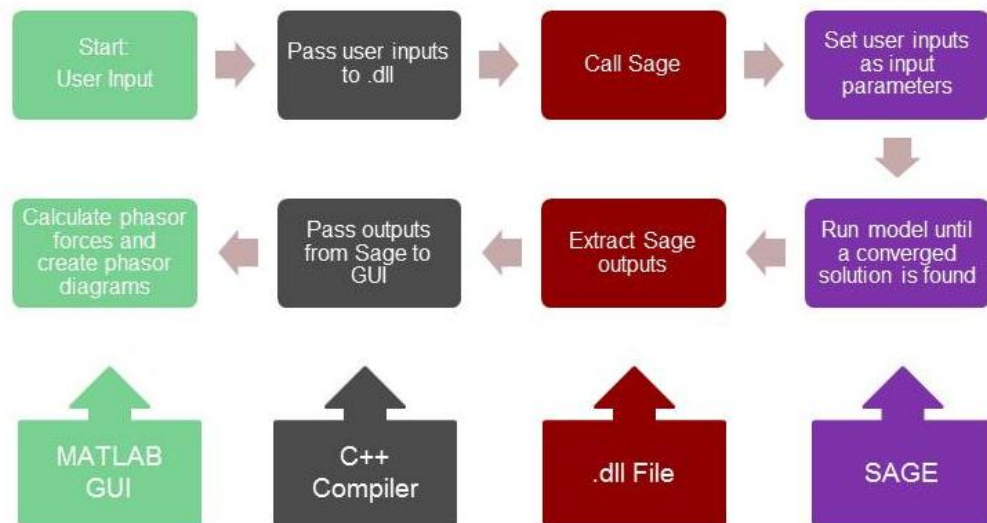


Figure 6. Diagram of interaction between MATLAB and Sage.

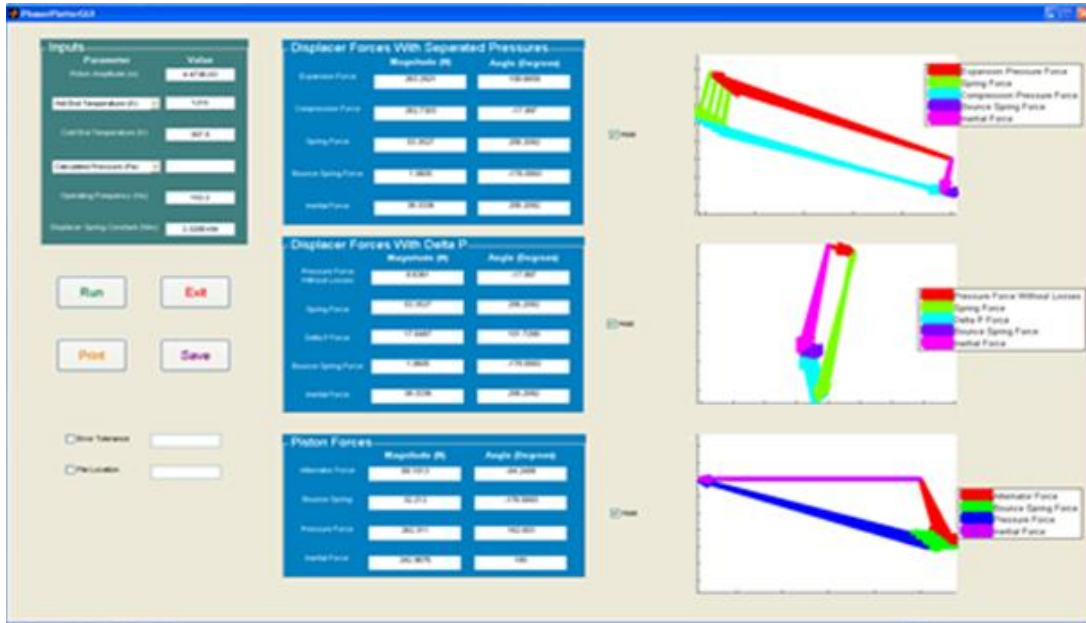


Figure 7. MATLAB GUI running Sage dll and creating phasor diagrams.

II. Linear Alternator Model Development

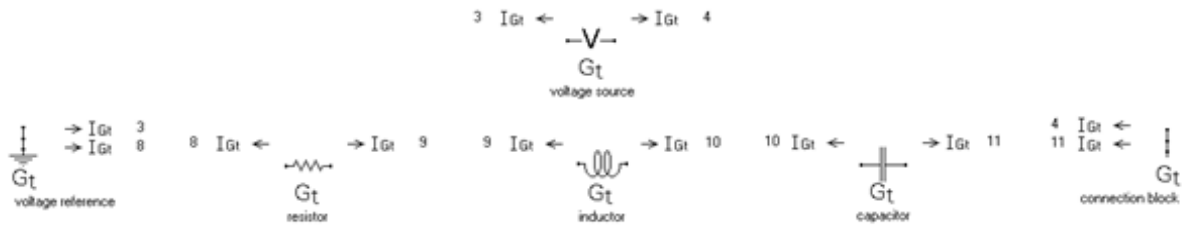


Figure 8. Example RLC circuit model in Sage.

Alternators could not be modeled with older versions of Sage software. The newest version of the Sage software (ver. 9.1) now includes electromagnetic model components. The electromagnetic model library includes basic electronic circuit components such as voltage and current sources, resistors, capacitors, and inductors. Figure 8 shows a basic RLC circuit model in Sage. It also includes components such as wire coil, permanent magnets, ferromagnetic material, magnetic flux sources, and magnetic field sources. These components can be used to develop simple circuit models or combined with mechanical components to create more complex parts such as alternators or linear motors. The components are connected in the same manner as the mechanical components. The components have only single input/output current interfaces, but may be connected to connection blocks or voltage references which can have multiple (user-defined) interface connections. It should be noted that all electromagnetic components are time-ring rather than phasor components. Another component of the library is labeled a “transducer.” This part largely ignores the physics of the interaction of mechanical force and electric current in an alternator and assumes the relationship shown in Eq. 1, where C_f is the measured motor constant. It also assumes ideal power transfer from the piston to the alternator by Eq. 2. In reality there is loss associated with the alternator. Although not as rigorous as developing an alternator model from basic components, this method does provide a simplified approach of developing an alternator model to test with the existing thermodynamic model of the ASC. This is useful for testing the integration of the two models as well as learning some of the idiosyncrasies of the Sage modeling system.

$$F = C_f * I \tag{1}$$

$$F dx/dt = \Delta VI \tag{2}$$

A. Linear Alternator

The linear alternator operates on the principle of Faraday’s law. Magnets are attached to a magnet can on the piston of the ASC such that they pass through the alternator coil as the piston reciprocates. The changing magnetic field through the alternator coil induces a voltage V_{emf} . The voltage generated is proportional to rate of change of magnetic flux ϕ through the coil (therefore proportional to the velocity of the piston) and proportional to the number of turns N in the coil (Eq. 3).

$$V_{emf} = -N \frac{d\phi}{dt} \tag{3}$$

The circuit diagram in Fig. 9 is a representation of the linear alternator elements and the AC bus controller. The coil of wire in the alternator has an inductance and resistance represented by L_{alt} and R_{alt} in the diagram. The resistors $R1$ and $R2$ represent the wire resistance of the circuit and the lead resistance, and are typically small values. The inductance of the alternator creates a voltage phase shift relative to the current which reduces the power factor. A tuning capacitor is used to correct the phase shift caused by the alternator inductance. The AC Power Supply (or AC bus voltage) is used to control the piston amplitude by applying a voltage back to the alternator. The magnitude of the AC bus voltage alters the alternator force on the piston thereby altering the piston amplitude and phase. It is important to model and understand this relationship to be able to achieve control and synchronization of both pistons in an ASRG.

The circuit can be solved simply by Kirchhoff’s voltage law to find the necessary AC bus voltage, however it is more useful to model this in Sage to see how circuit elements affect ASC performance. Figure 10 shows the linear alternator circuit in Sage using the transducer model component. A force input to the transducer (from a piston) is translated to a current. The amplitude and frequency of the piston determines

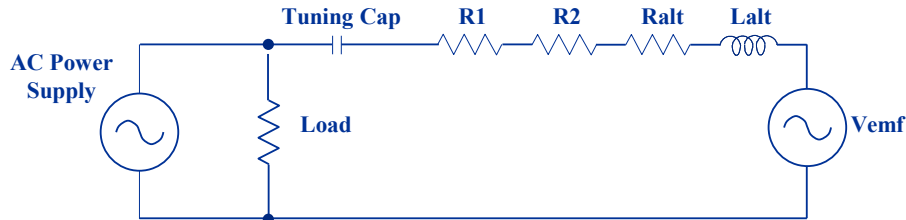


Figure 9. Circuit diagram of the linear alternator and AC bus controller.

the voltage generated.

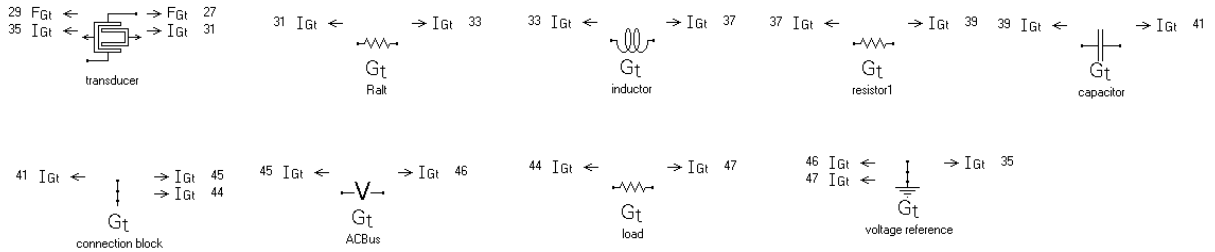


Figure 10. Linear alternator circuit model in Sage.

B. Model Integration

To form a complete model, the alternator needs to be combined with the ASC model, as shown in Fig. 11. The alternator model (Fig. 10) is inserted into the ASC Sage model (Fig. 5) and a force interface is added to the free-piston component in order to connect to the force interface of the transducer.

Unfortunately the transducer component does not consider any losses due to eddy-currents or hysteresis. To simulate some loss a damper was added and connected to the piston. While not entirely accurate, it is enough for development purposes and can be calibrated based on test data at a later point.

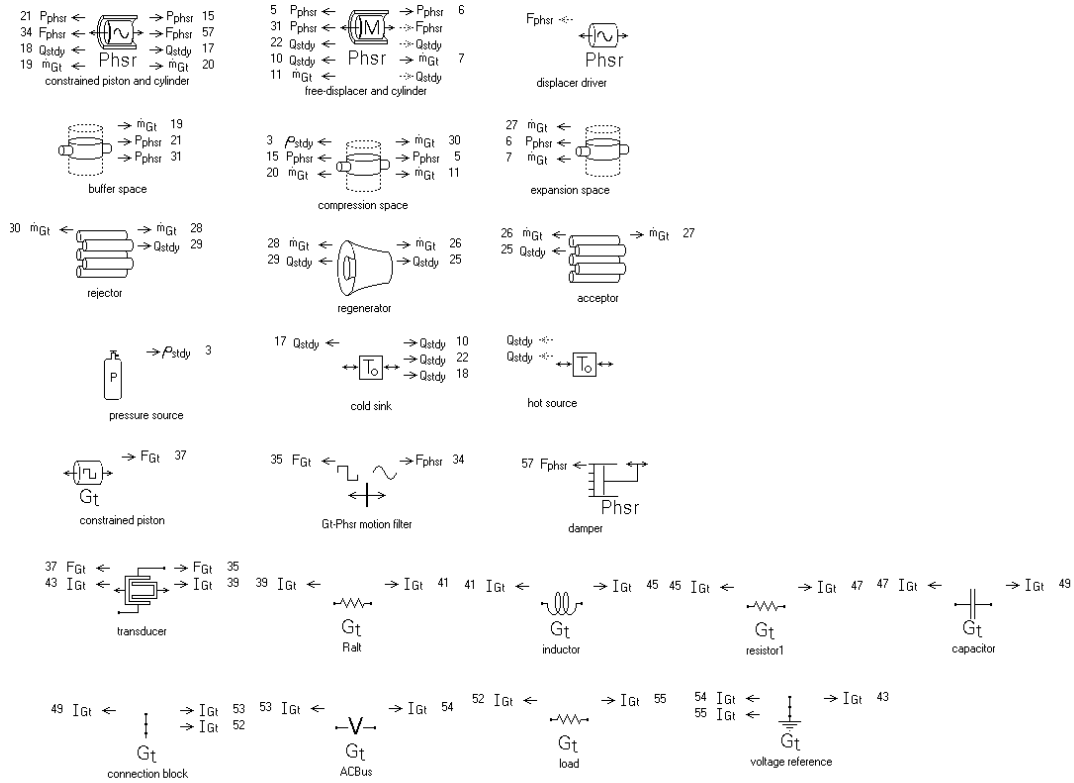


Figure 11. ASC constrained piston and linear alternator model.

The ASC model assumes a constrained piston (piston with set amplitude). This is not realistic but it is useful in determining system characteristics with a set piston amplitude. The piston amplitude is set as an input and system forces are calculated. Any required force necessary to keep the piston in motion at the given amplitude is calculated and output as a required forcing function (Fig. 12a). With the addition of the linear alternator model this can also be used as a sanity check on the model. The AC bus voltage is used to control piston amplitude; therefore the required forcing function should be driven to zero with a reasonable voltage input as shown in Fig. 12b.

To create a more realistic model the constrained piston component was replaced with a free-piston component. This allows the piston amplitude to vary based on system input parameters, including temperature variations of the system and AC bus voltage changes. Piston amplitude is now an output of the Sage solver rather than an input.

Outputs			
	F	boundary force (N, rad)	2.842E+02 cis(2.929)
	Wnet	boundary power inflow (W)	8.614E+01
a)	FF	required forcing function (N, rad)	6.944E+01 cis(-1.043)
Outputs			
	F	boundary force (N, rad)	2.429E+02 cis(-3.142)
	Wnet	boundary power inflow (W)	-1.809E-05
b)	FF	required forcing function (N, rad)	1.317E-05 cis(1.868)

Figure 12. a) Model output with a required forcing function (69.44 N). b) Model output with the required forcing function driven to near zero (1.809E-05 N).

C. Alternator Voltage Phasor Diagram

Using the new model of ASC and the Sage dll, the MATLAB GUI is able to run the model and collect the outputs to create a voltage phasor diagram of the linear alternator. Voltage amplitudes and phases are taken in by the GUI and vectors created in a head-to-tail method. The phase of the voltage through a resistor is the same as the phase of the current, hence the voltage R_{alt} is in phase with current. The phase of the current is considered to be along the x-axis in the voltage phasor diagram.

Figure 13 shows a typical voltage phasor diagram for the linear alternator. The voltage across the alternator resistance is in phase with the current, however the phasor is plotted in the opposite direction to indicate a voltage drop. The alternator inductance and tuning capacitance phasors are -90 and 90 degrees respectively as a result of this sign convention. The alternator voltage phasor is the voltage at the terminal leads and is the sum of the V_{emf} , alternator resistance, and alternator inductance phasors. This is useful to plot because the terminal lead voltage can be measured in testing while the V_{emf} , resistance, and inductance can only be calculated.

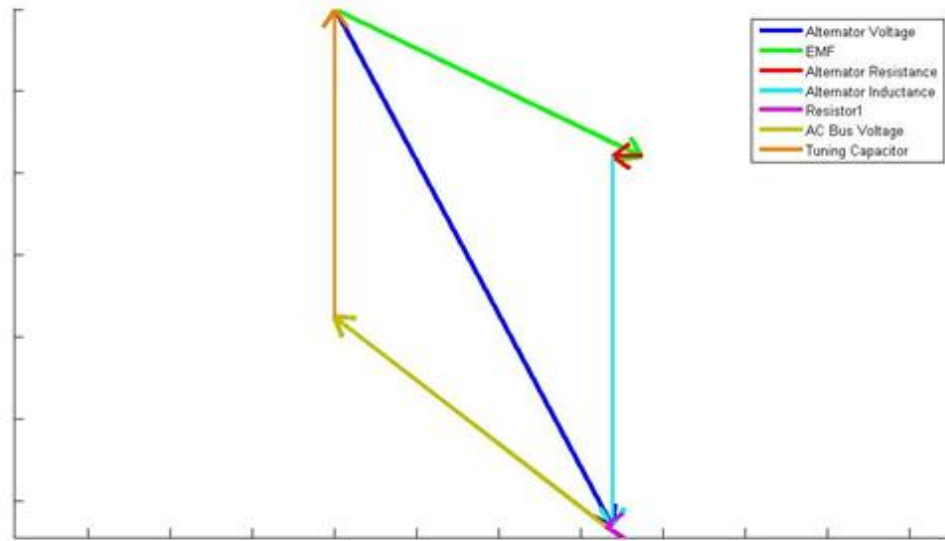


Figure 13. Voltage Phasor Diagram of the Linear Alternator

III. MATLAB GUI and Model Improvements

A new MATLAB GUI, shown in Fig.14, was developed to interface with the new Sage ASC model. The GUI expands the input panel to include linear alternator parameters. A main feature of the interface is the ability to set either AC bus voltage and solve for the resulting piston amplitude or vice versa. This capability is enabled by the newly integrated Sage model. Two phasor diagrams have been added to the original three (Piston Forces, Displacer Forces with Separated Pressures, and Displacer Forces with Delta Pressure). The phasor diagram of alternator voltages has been added along with corresponding output data. A phasor diagram depicting the phase of forces relative to the phase of the piston motion has also been added.

A. Improvements

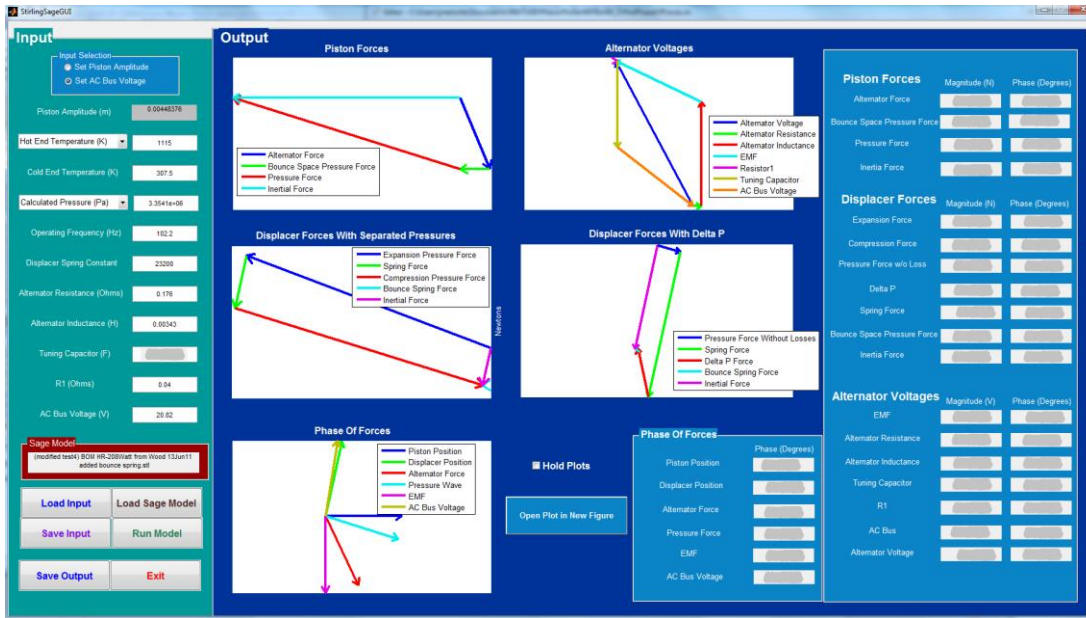


Figure 14. MATLAB GUI running Sage model and plotting phasor diagrams.

Other improvements have been made to the GUI such as the ability to save input and output data. The output data includes the force data in the output window as well as the Sage output data listing for the model. Previous input data can then be loaded to rerun a simulation. Phasor diagrams can be opened into separate figure windows for easier viewing and manipulation.

The heat input parameter has been improved to allow the user to specify the heat input of the heat source in watts instead of specifying the hot-end temperature. This can be useful to simulate the heat input of the GPHS. Sage however requires hot-end temperature in Kelvin as an input parameter. The net heat input to the convertor is not equal to the gross heat output from the GPHS. Some heat is lost to the insulation, leaving a net heat input ($Q_{in,net}$). An iterative process is used to determine $Q_{in,net}$ and the corresponding hot-end temperature. The hot-end temperature is estimated and input to Sage, which calculates as an output the heat input $Sage_{Q_{in}}$. This is compared to the calculated $Q_{in,net}$ which takes into account heat loss through insulation. The estimated hot-end temperature is adjusted based on the difference between $Sage_{Q_{in}}$ and $Q_{in,net}$ and the cycle is repeated.

B. Future Work

The new Sage model and MATLAB GUI offer increased capability over previous models, however there is still room for improvement. The linear alternator model does not accurately calculate alternator losses. The method currently used can change as input parameters are altered, but it is unknown if these changes accurately represent reality. The current model also is a very simple representation of the alternator. A better physical model could be developed in Sage utilizing the magnetic and coil components to build a more physical representation. This type of model in Sage may also be able to better model alternator losses. Another improvement is to combine two ASC models in Sage to develop an ASRG model, allowing a more complete simulation of the entire generator. Finally, the models need to be validated with test data to quantify their accuracy.

IV. Conclusion

The addition of the linear alternator and AC bus controller to the ASC model gives a more realistic representation of the system. It allows the piston amplitude to be determined based on the system input parameters while offering insight into how system performance is affected by changes to the AC bus voltage, which was not possible in the previous model. The reworked GUI complements the new model by simplifying the access to the Sage model parameters and providing quick insight into model performance

through phasor diagrams. This tool can be easily adapted and expanded to accommodate future model improvements and GUI enhancements.

Acknowledgments

This work was funded by the NASA Office of Education through the Undergraduate Student Research Program (USRP). Any opinions, findings, conclusions, or recommendations expressed in this article are those of the authors and do not necessarily reflect the views of NASA.

References

- ¹Richardson, R. and Chan, J., "Advanced Stirling Radioisotope Generator," Proceedings of NASA Science Technology Conference (NSTC 2007)
- ²Wood, J.G., Wilson, K., Buffalino, A., et al., "Continued Development of the Advanced Stirling Convertor (ASC)," *Proceedings of the 5th International Energy Conversion Engineering Conference (IECEC 2007)* American Institute for Aeronautics and Astronautics, 2007
- ³Walker, G and Senft, J.R. *Free Piston Stirling Engines*, Springer-Verlag, 1985.
- ⁴Shaler, K and Lewandowski, E.J., "Stirling Convertor Dynamic Analysis Using Phasor Diagrams", *Proceedings of Nuclear and Emerging Technologies for Space (NETS 2011)*
- ⁵Gedeon, David, "Sage: Object-Oriented Software for Cryo-cooler Design," *Cryocoolers 8*, Edited by R.G. Ross, Jr., Plenum Press, New York, pp. 281-292, 1995.
- ⁶Saha, Dipanjan, and Lewandowski, E.J., "Development of a Phasor Diagram Creator to Visualize the Piston and Displacer Forces in an Advanced Stirling Convertor," *Proceedings of Nuclear and Emerging Technologies for Space (NETS 2013)*

Appendix B

Appendix B contains the second conference paper titled, “Development and Validation of Linear Alternator Models for the Advanced Stirling Convertor.” This paper is authored by Jonathan Metscher and Edward Lewandowski and is anticipated to be published in the Proceedings of the Twelfth International Energy Conversion Engineering Conference (IECEC 2014), American Institute for Aeronautics and Astronautics, in Cleveland,OH.

Development and Validation of Linear Alternator Models for the Advanced Stirling Convertor

Jonathan F. Metscher¹ and Edward J. Lewandowski²
NASA Glenn Research Center, Cleveland, OH 44135

Two models of the linear alternator of the Advanced Stirling Convertor (ASC) have been developed using the Sage 1-D modeling software package. The first model relates the piston motion to electric current by means of a motor constant. The second uses electromagnetic model components to model the magnetic circuit of the alternator. The models are tuned and validated using test data and compared against each other. Results show both models can be tuned to achieve results within 7% of ASC test data under normal operating conditions. Using Sage enables the creation of a complete ASC model to be developed and simulations completed quickly compared to more complex multi-dimensional models. These models allow for better insight into overall Stirling convertor performance, aid with Stirling power system modeling, and in the future support NASA mission planning for Stirling-based power systems.

Nomenclature

ASC	=	Advanced Stirling Convertor
B_r	=	residual magnetic flux density (T)
BOM	=	beginning of mission
K_i	=	alternator motor constant (N/A)
EM	=	electromagnetic
EOM	=	end of mission
F	=	Force (N)
FringeMult	=	Sage fringe effect multiplier
HR	=	high reject temperature
I	=	current (A)
J_{sat}	=	saturation magnetic polarization (T)
Jmult	=	Sage magnet strength multiplier
L_{alt}	=	alternator inductance (H)
LR	=	low reject temperature
N	=	number of turns
PM	=	permanent magnet
Q	=	net heat input (W)
R_{alt}	=	alternator resistance (Ω)
$R1, R2$	=	resistances (Ω)
$Sage_{Q_{in}}$	=	net heat input as calculated by Sage (W)
V_{emf}	=	electromotive force (EMF) voltage (V)
Wnet	=	Power (W)
x	=	position (m)
μ_r	=	relative magnetic permeability (N/A ²)
ΔV	=	voltage (V)
Φ	=	magnetic flux (Wb)

¹ Coop Student, Thermal Energy Conversion Branch, 21000 Brookpark Rd.

² ASRG Project Lead Engineer, Thermal Energy Conversion Branch, 21000 Brookpark Rd., AIAA Senior Member.

I. Introduction

STIRLING technology development¹ is continuing at the NASA Glenn Research Center (GRC) as an efficient and reliable power system potentially for NASA's deep space missions. Currently, when radioisotope power is required, NASA deep space missions use radioisotope thermoelectric generators (RTGs), which convert the heat from radioactive decay of Plutonium-238 into electric power, but they have efficiencies of 5 to 7 percent. Stirling engines are a higher-efficiency alternative that could significantly reduce the amount of material used in radioisotope power systems by a factor of 4 or more.^{1,2}

The Advanced Stirling Convertor^{3,4} (ASC), developed by Sunpower, Inc., is a free-piston Stirling engine coupled with a linear alternator. The ASC is currently under extended testing at GRC.^{5,6} It is a reciprocating resonant system that consists of a helium filled pressure vessel containing a piston, displacer, and linear alternator. Electrical power is extracted in the linear alternator where the reciprocating piston motion drives magnets through the alternator coil. Figure 1 is a cross section view of a generic free-piston Stirling convertor and defines the main components.

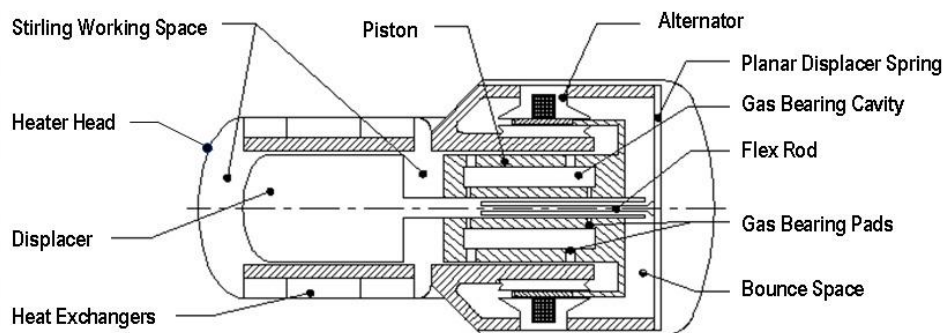


Figure 1 : ASC Cross Section Layout

A. ASC Modeling

Modeling and simulation is important in the development and testing of Stirling engines as it aids in optimization of design, analysis of system performance, and understanding of physical parameters that are impractical to measure in Stirling devices. There have been both one-dimensional (1-D) and multi-dimensional modeling and simulation efforts focusing on the ASC. One-dimensional models use nodes to directly solve the governing system equations and are advantageous due to their fast computation times and ease of setup.⁷ One-dimensional models such as the System Dynamic Model⁸ (SDM) enable whole convertor simulation by linking representative elements within the Simplorer™ commercial software package. SDM also has capability of modeling transient startup and non-linear dynamic behavior, although this makes it more computationally intensive. SDM is limited by less sophisticated Stirling cycle thermodynamics and a simplified alternator model. Sage is another 1-D modeling package that is used to model Stirling engines. It is a steady state modeling package that is less computationally intensive and has been continually improved over the years. Its thermodynamic computations have been shown to agree well with 2-D computational fluid dynamic (CFD) models.^{9,10} Recent additions to the Sage model library allow for modeling of linear motors and alternators, enabling whole convertor modeling of the ASC. Further detail on Sage and validating its modeling capability is discussed later in this paper.

Multi-dimensional simulations are typically CFD models that focus on specific regions of the Stirling engine such as the regenerator, although there has been some work toward whole engine modeling.⁷ Multi-dimensional simulations offer many advantages as outlined by Dyson¹¹, such as modeling inherently 3-D phenomena as flow turbulence. Multi-dimensional simulations are computationally expensive and do not typically include linear alternator modeling to give a whole convertor simulation. The ANSYS Maxwell finite element method (FEM) software package allows multi-dimensional modeling of the linear alternator and has been used at GRC to model linear alternator designs from earlier Stirling convertor efforts.¹² Maxwell has the same disadvantage of being computationally expensive and not able to model the whole convertor.

A whole convertor model would be beneficial in analyzing test data as it enables the simulation of parameters that are impractical, if not impossible, to measure and assists in system verification and validation. This paper reviews a whole convertor modeling effort using the Sage software package. As a 1-D model, it will allow for fast development and simulation times. Simulations are compared to test data to validate the model and determine model limitations.

B. Sage Overview

Sage¹³ is a 1-D Stirling device modeling software package developed by Gedeon Associates. Sage contains a library of generic model components that can be placed and connected in the Sage graphical user interface (GUI). The model components contain the user-defined dimensions and properties and are connected to other model components through various connection interfaces (force, pressure, volume flow, heat flow, etc.). Sage components can be thought of as building blocks that are assembled to form the system of interest.¹⁴ Figure 2 shows an example of Stirling engine components and their interconnections. Components may then have sub-components and their own connections. This modular method facilitates quick model construction as the underlying equations are defined by the components and their interconnections. Sage allows the user to optimize parameters according to defined constraints and optimization objectives. This powerful ability enables design optimization or can assist in tuning model parameters using performance data.

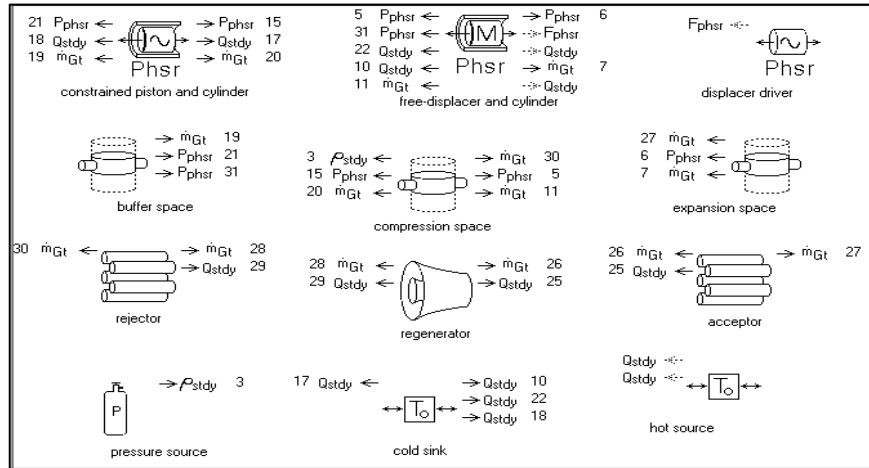


Figure 2: Sage Stirling engine model.

The Sage library is divided into model classes (Stirling, Pulse Tube, and Low-T Cooler). The Stirling model class has been used for modeling ASC engines, but until recently was unable to model the linear alternator. The recent addition of electromagnetic (EM) components to the Sage library allows the modeling of simple circuits and linear motors and alternators, enabling whole convertor modeling of the ASC.

The Sage EM library consists of basic circuit components as well as magnetic components. It includes resistor, capacitor, and inductor model components as well as voltage and current sources. Component properties are user-defined and the components are connected through current interfaces. These components can be used to model simple RLC circuits as shown in Fig. 3, or used as part of more complex EM models and combined with magnetic model components.

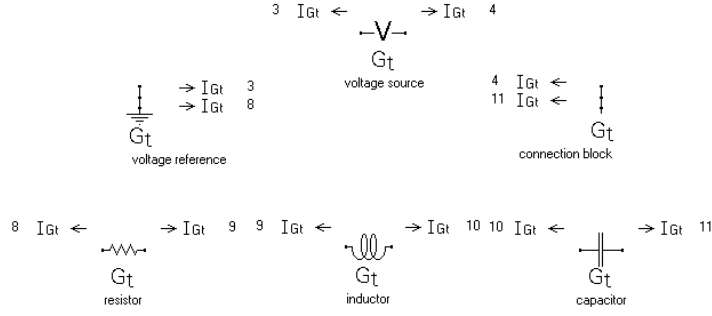


Figure 3: Example RLC circuit model in Sage.

The library also includes a wire coil that can be used with magnetic model components to develop linear electric actuator and generator models or similar devices such as transformers. The library contains magnetic components such as magnetic field or flux sources, air gaps between magnetic components, permanent magnet (PM) and ferromagnetic materials, and magnetic single- or two-pole components. EM components are connected through magnetic flux (ϕ) interfaces. Some of these high-level components have built-in sub-components to further define the model structure. The user defines the physical dimensions of the components, however it should be remembered that this is a 1-D model and the geometry is assumed axisymmetric. The solution is also time-periodic and does not model transient behavior, making this unsuitable for certain system simulations or analyses.

C. Linear Alternator Operation

A linear alternator operates on the principle of Faraday's law in which an electromotive force (emf), or voltage, is induced along the boundary of a surface through which there is changing magnetic flux.¹⁵ In the case of the ASC linear alternator, permanent magnets are attached to the piston which oscillates within the alternator coil. The magnetic field (B) from the magnets is directed across the pole gaps and through the inner and outer ferromagnetic cores, following a path of least reluctance (\mathfrak{R}) much like current through circuit follows a path of least resistance. As the piston moves through one cycle, the magnetic flux changes as its path changes. The magnetic flux passing through the alternator coil will increase and decrease in an oscillatory manner due to the changing position of the magnets within the stationary ferromagnetic cores, causing the magnetic field to change direction. This changing magnetic field passing through the circular surface enclosed by the alternator coil causes a voltage to be induced (V_{emf}). Equation (1) shows Faraday's law in its integral form. Magnetic flux (ϕ) is the integral of the magnetic field through a surface (Eq. (2)) and the magnetic flux through each "surface" created by the turns (N) of the alternator coil are known as flux linkages ($N\phi$).¹⁶ V_{emf} can be simplified as the time derivative of the flux linkages (Eq. (3)).

$$V_{emf} = -\frac{d}{dt} \int \vec{B} \cdot \hat{n} da \quad (1)$$

$$\phi = \int \vec{B} \cdot \hat{n} da \quad (2)$$

$$V_{emf} = -N \frac{d\phi}{dt} \quad (3)$$

V_{emf} is in phase with piston velocity; however, the voltage at the alternator terminals (V_{alt}) is phase shifted due to the inductance of the coil and acts to oppose changes in current. This behavior stems from Lenz's law in which the direction of the induced current in the coil flows as to create a magnetic field

opposing the change in magnetic flux through the coil. Inductance (L) is defined in Eq. (4)¹⁷. Sage takes a slightly different approach at calculating inductance (Eq. (5))¹⁴ but can be shown to be consistent by substituting the relationship between voltage and inductance shown in Eq. (4).

$$L = \frac{d\phi}{dI} = - \frac{V_{emf}}{\frac{dI}{dt}} \quad (4)$$

$$L = - \frac{\phi \Delta V * I}{\phi \dot{I}^2} \quad (5)$$

II. Linear Alternator Modeling Using Sage

A. Sage Linear Alternator Modeling Using the Sage Transducer Component

An alternator model can be created using the “transducer” component (Fig. 4) in the Sage EM library. Like a physical transducer, it converts energy from one type to another. In Sage it converts mechanical energy to electrical. The component has built in force and current connections and assumes the relationship shown in Eq. (6) and energy conservation shown in Eq. (7). The variable K_i is user-defined to match the system characteristics. In a linear motor or alternator type model, K_i is the motor constant.

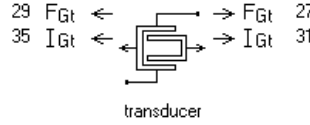


Figure 4: Sage Transducer Component

$$F = K_i * I \quad (6)$$

$$F dx/dt = \Delta VI \quad (7)$$

1. Transducer Alternator Model Components

Figure (5) shows a circuit diagram of a linear alternator with controlling circuit elements. V_{emf} represents the voltage generated by the linear alternator while R_{alt} and L_{alt} represent the resistance and inductance of the alternator, respectively. The remaining resistors R1 and R2 are the wire and lead resistance in the circuit. A tuning capacitor is used for power factor correction and an AC power supply controls the piston amplitude. This circuit diagram is a useful comparison to the Sage model of a linear alternator using the transducer component described earlier. Figure (6) shows a Sage model of a linear alternator.¹⁸ The model requires three key Sage EM components to model the linear alternator. The primary component is the transducer that converts force from the piston into electric current; however, it does not account for the resistive and inductive properties of the wire coil in the alternator. A resistor and an inductor component are needed to account for these properties. The outlined components show the key linear alternator components. The remaining components model the rest of the circuit connected to the linear alternator and compare directly to the circuit diagram.

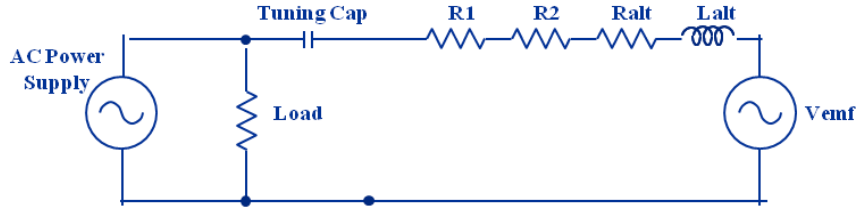


Figure 5: Circuit diagram of the linear alternator and AC bus controller.

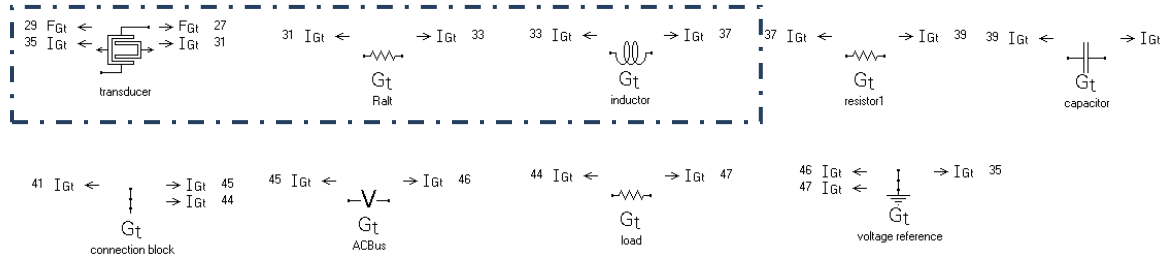


Figure 6: Linear alternator circuit model in Sage using the transducer component. Outlined are the main linear alternator model components.

2. Transducer Alternator Model Tuning

This method of modeling a linear alternator is simple to implement, requiring only three components, but is limited in that it ignores the underlying physical phenomena and potential losses such as eddy-currents, hysteresis, and flux leakage. It also requires that the user have data to input properties such as alternator inductance and resistance as well as the motor constant K_i . For the ASC, values for alternator inductance and resistance are known. In an attempt to account for losses, an additional resistor R_{loss} is added in the Sage model, though this assumes the losses are proportional to current. Determining an appropriate resistive loss is not straightforward as the real losses may change with convertor operation point. The same could be true for K_i .

The Sage optimization tool can be used to investigate appropriate values for R_{loss} and K_i . An estimate value for both can be input into Sage and then set as optimization variables. Constraints can be set on output variables and an objective function defined for Sage to achieve by varying the values of R_{loss} and K_i . Using performance data from the ASC, current and voltage output values are constrained to be within 2.5% of measured values and the objective function set to match the measured power factor. This was performed at four boundary operating points for the ASC known as beginning of mission (BOM) and end of mission (EOM) with high and low reject (HR and LR) temperatures at each case. The results of these optimization cases show the values for R_{loss} and K_i vary slightly across the four operation points, but a correlation can be made with the K_i value and rejection temperature (Fig. 7). This is not unexpected as the transducer and R_{loss} components do not model changes in performance due to temperature. Using this correlation, the value of K_i was input into Sage as a function of rejection temperature and the simulation repeated over the test points.

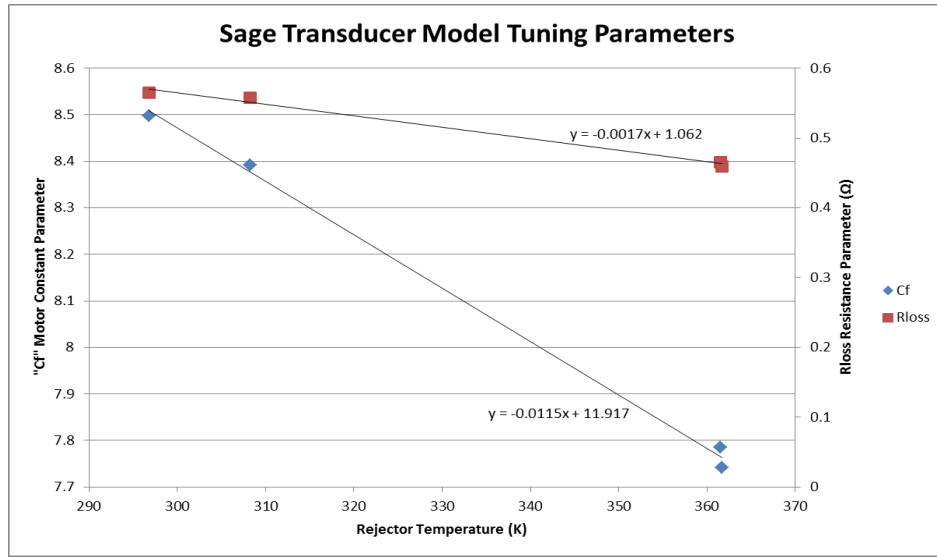


Figure 7: Transducer Tuning Parameter Value as a Function of Rejector Temperature

B. Sage Linear Alternator Modeling with Electromagnetic Components

Creating a linear alternator model with EM components is more complex than the “transducer model”, but offers the advantage of modeling the physical characteristics of the system from first-principles. The high-level Sage EM components that model the linear alternator include a two-pole magnetic gap, a wire coil, ferromagnetic cores, and magnetic reference and connection blocks. These components are generated with the necessary magnetic flux boundary interfaces and are connected as shown in Fig. 8. The component layout in Sage does not visually represent a linear alternator, so it is important to understand the underlying physics that Sage is attempting to model.

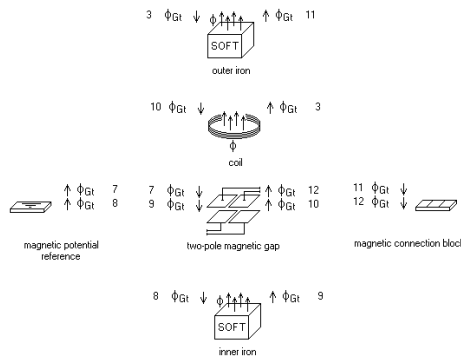


Figure 8: Sage Linear Alternator High-level Components

1. Sage EM model connections and solution method

Magnetic components such as permanent magnets, magnetic poles or gaps, and ferromagnetic materials are connected through magnetic flux (ϕ) boundary interfaces that are a function of the magnetic potential difference (or magneto-motive force) across each component. Each component defines the relationship between magnetic flux and magneto-motive force based on the magnetic properties of the component. The wire coil component has both current and magnetic flux connections and the magnetic pole components have both force and magnetic flux connections. These components make it possible to model energy conversion from mechanical to EM and enable whole convertor modeling.

The Sage solution framework for EM models is based on a magnetic circuit approach. If the magnetic flux within a system is confined to a well-defined path, then the system may be understood as a magnetic circuit¹⁷, analogous to current confined to wires and components in electric circuits. Table I lists the key magnetic properties and their corresponding analogous electric properties.

Table I: Magnetic and Electric Analogous Terms

Magnetic Property	Electric Property
\mathcal{F} = Magneto-motive force (mmf) (Amp-turns)	V = Electromotive force (emf) (V)
ϕ = Magnetic flux (Wb)	I = Electric current (A)
\mathcal{R} = Magnetic reluctance (H^{-1})	R = Electric Resistance (Ω)
μ = Permeability	σ = Conductivity

In the magnetic circuit analogy, the magnetic system can be modeled as an electric circuit. Figure 9 shows an EM system and its corresponding electric circuit. In this example the coil produces the magneto-motive force \mathcal{F} and a magnetic flux ϕ “flows” through the system. It should be noted that “flow” is merely a continuation of the electric circuit analogy as current flows through a circuit, but nothing is actually flowing through the magnetic system. The reluctance in the magnetic system due to the ferromagnetic core and air gap are analogous to resistors in an electric circuit. With this analogy, the system model can be solved using Eq. (8), which corresponds to Ohms law.

$$\mathcal{F} = \phi \mathcal{R} \quad (8)$$

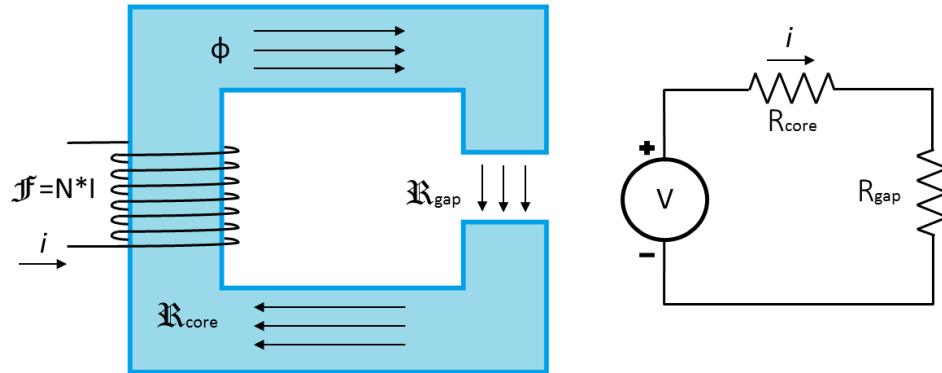


Figure 9: Magnetic Circuit Analogy

2. Properties of Sage EM Components and Sub-components

The input properties of the Sage EM components are based on the basic geometry of the alternator and relationship between components. Figure 10 shows the generic axisymmetric structure assumed in the Sage alternator model. The two-pole magnetic gap component defines the overall framework of the alternator including the length of the poles, separation between poles (x directed, along the axis), and the magnetic gap between pole faces (z directed, perpendicular to the axis). Sub-components with the two-pole component include an “EM container” which can hold permanent magnet or ferromagnetic component (for moving magnet or moving iron types of magnetic systems). The sub-components model the magnetic material, dimensions, and initial conditions such as temperature and position. Along with the magnetic flux interfaces generated from the magnetic poles is a force interface to the magnet (EM container) to connect with force interface of the piston.

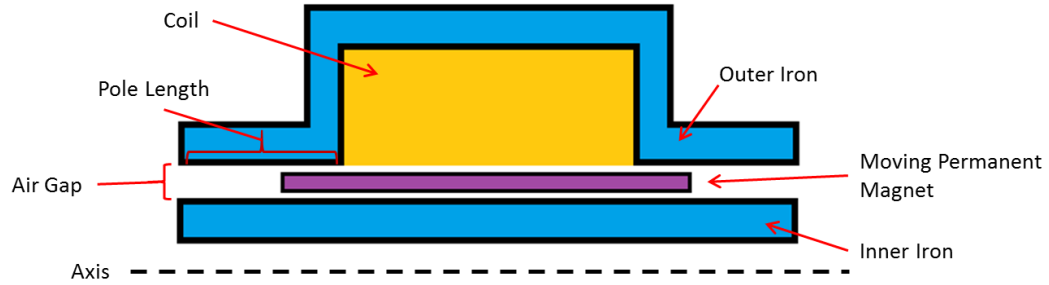


Figure 10: Linear Alternator Generic 2-D Cross Section Assumed by Sage

The inner and outer iron components in the model are based on the ferromagnetic material used for the alternator core and its effective magnetic path length and area. The coil component models the physical coil wire parameters such as number of turns, wire cross-sectional area, coil cross-sectional area, and coil average diameter. Coil resistance is an output parameter calculated based on wire dimensions, material properties and temperature. Coil inductance is also an output parameter that is calculated (Eq. (8)) rather than being an input parameter. The inductance can be shown to be governed by the physical dimensions of the coil and magnetic properties of the iron core. In the case of the alternator, the coil area is constant and the magnetic flux linkage can be simplified to Eq. (9) where “A” is the area of the coil and “l” is the length of the coil. The inductance of the alternator can then be defined by its physical properties (Eq. (10)) from its initial definition (Eq. (4))¹⁷.

$$\varphi = \frac{\mu N^2 A}{l} I \quad (9)$$

$$L = \frac{d\varphi}{dI} = \frac{\mu N^2 A}{l} \quad (10)$$

3. Sage EM Material Properties

The Sage EM library includes a selection of ferromagnetic and permanent magnet materials with typical material properties. Material properties can be edited or new materials added based on the requirements of the model. The manner that material properties are defined in Sage and assumptions made about the materials are important to the performance of the model.

Permanent magnet material properties are defined by the intrinsic (J(H)) and normal (B(H)) demagnetization curves as show in Fig. 11, where J is magnet polarization (SI unit Tesla), B is the magnetic flux density (SI unit Tesla), and H magnetizing force (SI unit Amperes per meter). Sage uses the J(H) curve end points (residual magnetic flux B_r and magnetization coercive force H_{cj}) as inputs and uses a curve fitting term to match the demagnetization bend. Magnetic characteristics are temperature dependent so Sage allows inputs at multiple temperature points and otherwise assumes a linear relationship based on the Curie temperature.

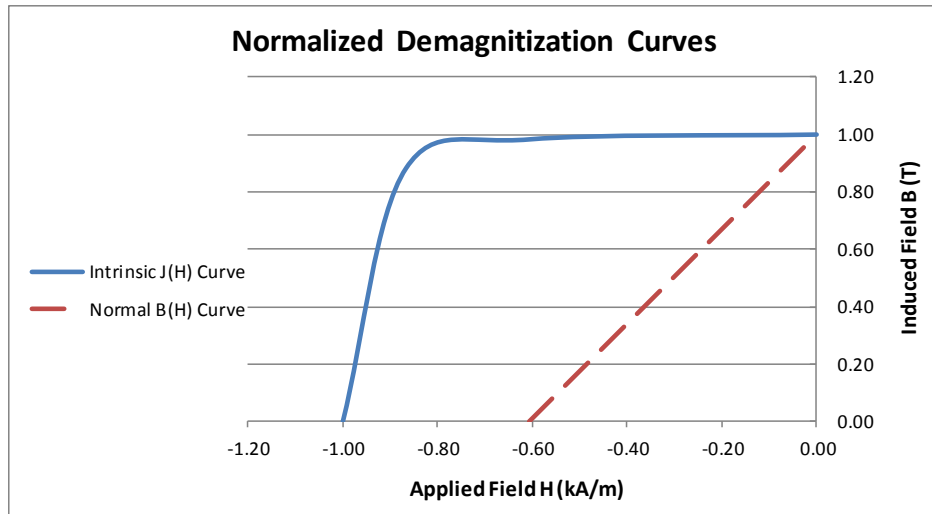


Figure 11: Permanent Magnet Demagnetization Curves (second quadrant of hysteresis loop)

Sage defines ferromagnetic material properties similarly to PM materials using critical points of the $J(H)$ curve of the material. The saturation magnetic polarization (J_{Sat} , SI unit Tesla) and the induction coercive force (SI units Amperes per meter) are input at a specified temperature. Multiple points can be input for different temperatures if the data exist, otherwise Sage assumes a linear decrease to zero at the Curie temperature. The maximum relative permeability (μ_r) is also specified. Sage provides ferromagnetic material $B(H)$ mapping model to allow comparison and tuning of the $B(H)$ curve of the material. Figure 12 shows a comparison of the $B(H)$ curve from test data and the $B(H)$ curve generated in Sage from data. This comparison allows for a “tuned” value for μ_r and J_{Sat} to be found and the $B(H)$ curve to be matched.

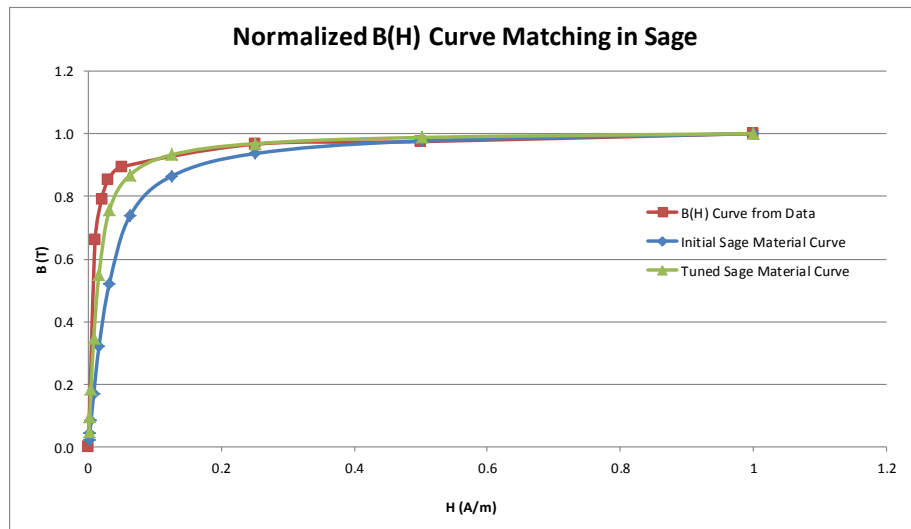


Figure 12: $B(H)$ Curve Matching in Sage for Ferromagnetic Core Material

C. Sage EM Alternator Model Tuning

The Sage alternator model is a 1-D model and assumes all input geometry is symmetric about its axis. This assumption works well but is not entirely accurate as manufacturing and assembly constraints can cause some non-symmetric features, such as the outer iron core laminations not forming a continuous covering. The dimensions of the alternator are also idealized as shown previously in Fig. 10. Actual alternator geometry is more complex. This may produce some inaccuracies due to Sage overestimating or underestimating parameters such as amount of iron core material and magnetic path length and area. This

can affect the magnetic circuit model by altering the magnetic reluctance of components or altering magnetic flux through components by inaccurate area calculations.

Another source of error in the EM model is from magnetic fringe field effects across the magnetic gaps at the poles of the alternator. Fringing flux occurs at gaps in the ferromagnetic path allowing the magnetic field to bulge outwards. Sage models fringing flux similarly to an electric field in a parallel plate capacitor, as the governing equations are similar and fringe fields in capacitors are well studied.¹⁴ It is also possible that not all of the windings of the alternator coil enclose the same amount of magnetic flux as Sage assumes. Figure 13 shows a 2D plot of flux through an alternator (created with the Maxwell FEM software package) with the PM off-center, showing the presence of fringing fields and field lines in the inner core not uniformly distributed along the length of the coil windings.

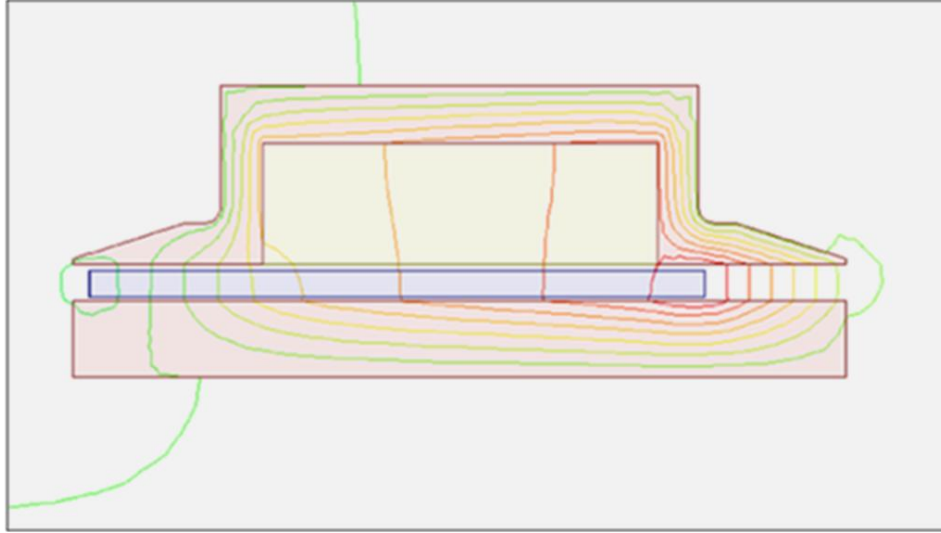


Figure 13: 2-D Magnetic Flux Plot of a Linear Alternator

1. Tuning Parameters

Sage has two built-in tuning parameters to address the known limitations of modeling using the EM components. There is a multiplier parameter “FringeMult” that directly scales the effect of fringing fields at the magnetic poles of the model. There is a second multiplier term “Jmult” that scales the strength of the PM. This can account for any demagnetization that may have occurred to the magnet during operation or reflect real magnet strength values less than those presented in the material data sheet. These terms together may also act to correct for other modeling inaccuracies such as geometry or magnetic flux path idealizations.

Certain parameters may also be altered in tuning of the alternator model to compensate for some of the inaccuracies in the model. The overall magnetic path length and area of the alternator may be modified to reflect the effective area of the iron cores that may not be accurately modeled in the axisymmetric assumption. Another possible parameter that could be used is the air gap dimension defining the distance between pole faces. Altering this distance (l_{gap}) changes the magnetic reluctance of the magnetic circuit as seen in Eq. (11).

$$\mathfrak{R} = \frac{l_{gap}}{\mu A} \quad (11)$$

2. Alternator Model Inductance Test and Verification

The inductance of the alternator directly impacts performance and is governed by the overall geometry of the coil and iron cores. Testing and tuning the Sage alternator model to match the measured inductance of alternator acts to increase confidence in the model’s physical parameters. As the coil parameters

(number of turns, resistance, dimensions, etc.) are well known and modeled accurately, it is the permeance (inverse of reluctance) of the magnetic path that may require tuning. The relationship between inductance and reluctance in a magnetic circuit (Eq. (12)) can be shown by substituting Eq. (4) into Eq. (5) and simplifying.

$$L = \frac{N^2}{\mathfrak{R}_{total}} \quad (12)$$

To check the inductance of the alternator model, a separate model was created with the identical alternator inputs. This alternator model was set up with a current source attached to the alternator and the piston stationary with magnets centered in the alternator. This was to mimic the inductance test performed on the linear alternator during the manufacturing process. A large current was input in the model and the inductance was reported in the Sage output listing.

3. Alternator Model Performance Tuning using Maxwell Model Simulation

The performance of the Sage EM alternator model was compared against a Maxwell FEM model of the alternator. This comparison served to examine the accuracy of a 1-D Sage EM model compared to the 3-D FEM model as well as to provide simulated alternator performance data for tuning purposes, in the absence of stand-alone alternator test data. The main tuning parameter tested in this process was the “Jmult” term. This tuning was re-evaluated in the integrated ASC model, combining the new Sage EM alternator model with the Stirling engine model, and the “Jmult” term adjusted.

III. Simulation Results and Model Validation

The Sage transducer model and EM model were combined with the ASC model and tuned at four key operating conditions (BOM-LR, BOM-HR, EOM-LR, and EOM-HR). Simulations using the tuned models at these operating points were compared to measured data from convertor verification testing conducted at Sunpower. After convertor verification testing at Sunpower, the position sensor attached to the displacer was removed before the ASC was placed on extended testing at NASA GRC. This slightly changes the mass of the displacer, so displacer mass in the Sage model was adjusted and simulations were compared to performance map tests conducted at GRC.

A. Sage ASC with Transducer Alternator Model Results

Table II displays the parameters measured, the BOM and EOM operating conditions, and the percent error between the tuned Sage ASC with transducer alternator model simulation and measured data points. Piston amplitude was matched as an input parameter for each case. The model agrees with measured data within 5% or better on most parameters.

Table II: Sage Transducer Model Percent Error to Test Data, BOM/EOM Point Comparison

Test Parameters Sage Transducer Alternator Model	BOM-LR	BOM-HR	EOM-LR	EOM-HR
Net-heat input, Q (W)	2.29%	-2.14%	5.37%	-2.36%
Piston Amplitude (mm)	0.00%	0.00%	0.00%	0.00%
Displacer Amplitude (mm)	0.73%	1.30%	0.82%	0.85%
Displacer to Piston Phase (degree)	1.01%	0.11%	2.03%	0.38%
Piston to Current Phase (degree)	-0.11%	2.30%	-1.51%	1.92%
Terminal power (W)	-0.27%	0.38%	0.64%	-0.46%
Power factor	0.21%	-0.43%	0.25%	0.30%
Voltage rms (V)	-2.64%	-2.43%	-1.18%	-2.78%
Current rms (A)	2.08%	2.38%	2.01%	2.37%
Efficiency (%)	-2.51%	2.58%	-4.49%	1.95%

The model was updated to include the change in displacer mass and simulations compared to performance map data performed at GRC. Figure 14 shows convertor efficiency at constant input

temperature and varied rejector temperature. Piston amplitude was also varied in the test data. The Sage model was operated at the same input temperature and piston amplitude as the test data. The values beside each data point are the net heat input, Q . The Sage model trends similarly with a net heat input difference less than +5%. Figure 15 show the same performance map data set plotted as power output vs. rejector temperature. It can be seen here the Sage model under predicts power output by 3%. The model's under prediction of power output and over prediction of heat input leads to the variance seen in conversion efficiency.

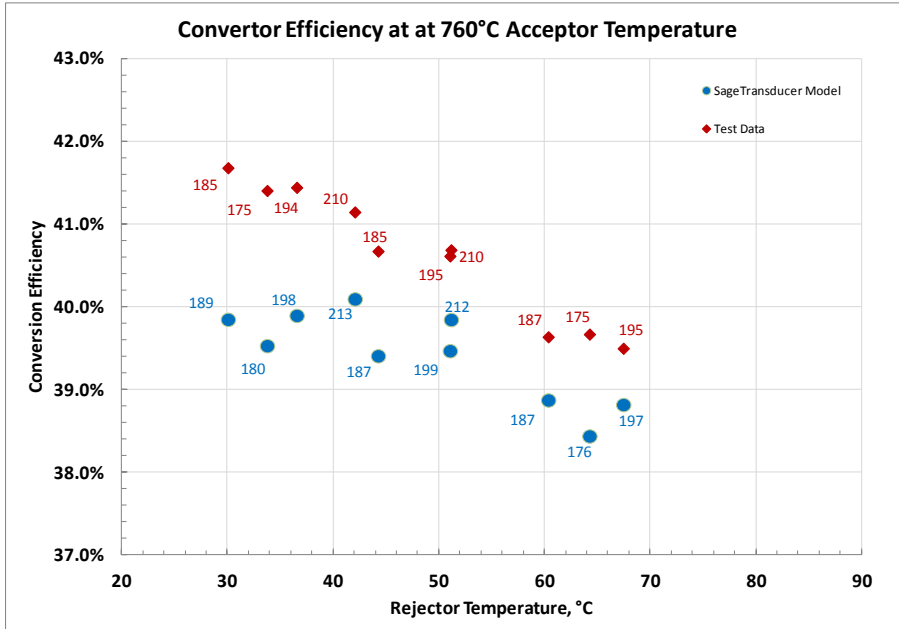


Figure 14: Sage ASC Model with Transducer Alternator, Comparison of Convertor Efficiency

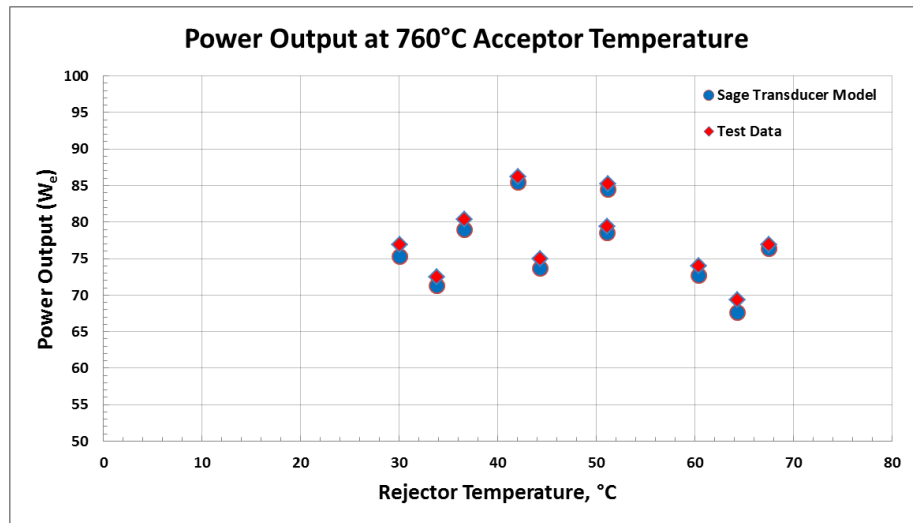


Figure 15: Sage ASC Model with Transducer Alternator, Comparison of Power Output

B. Sage ASC with EM Alternator Model Results

The Sage ASC model with EM alternator is operated at the BOM and EOM operating conditions and compared with measured data. Table III displays the parameters measured at the BOM and EOM operating conditions and the percent error between the model simulations and measured data. Acceptor and rejector

temperatures were set as inputs and piston amplitude was matched within 0.05%. The model was tuned at the BOM-LR operating conditions and agreed with measured data within 2%. The model agrees with the remaining operating points within 6% or better.

Table III: Sage EM Model, BOM/EOM Point Comparison

Test Parameters Sage EM Alternator Model	BOM-LR	BOM-HR	EOM-LR	EOM-HR
Net-heat input, Q (W)	-1.03%	-5.07%	1.92%	-5.45%
Piston Amplitude (mm)	0.00%	0.05%	-0.05%	-0.05%
Displacer Amplitude (mm)	-1.40%	-0.92%	-1.36%	-1.56%
Displacer to Piston Phase (degree)	-0.89%	-1.26%	-0.02%	-0.94%
Piston to Current Phase (degree)	0.44%	1.87%	-0.80%	1.92%
Terminal power (W)	0.44%	-3.96%	3.92%	-4.72%
Power factor	0.46%	1.45%	-0.63%	3.43%
Voltage rms (V)	-0.85%	-5.02%	2.57%	-5.32%
Current rms (A)	0.89%	-1.75%	1.70%	-2.37%
Efficiency (%)	1.48%	1.16%	1.96%	0.77%

The model was updated to account for the change in displacer mass and simulations compared to performance map data gathered at GRC. The simulations matched the acceptor and rejector input temperatures and piston amplitude. Figure 16 shows the convertor efficiency with varied rejector temperature and piston amplitude. Net heat input, Q, is displayed next to each data point. Convertor efficiency in the model simulations corresponds to test data within 2%.

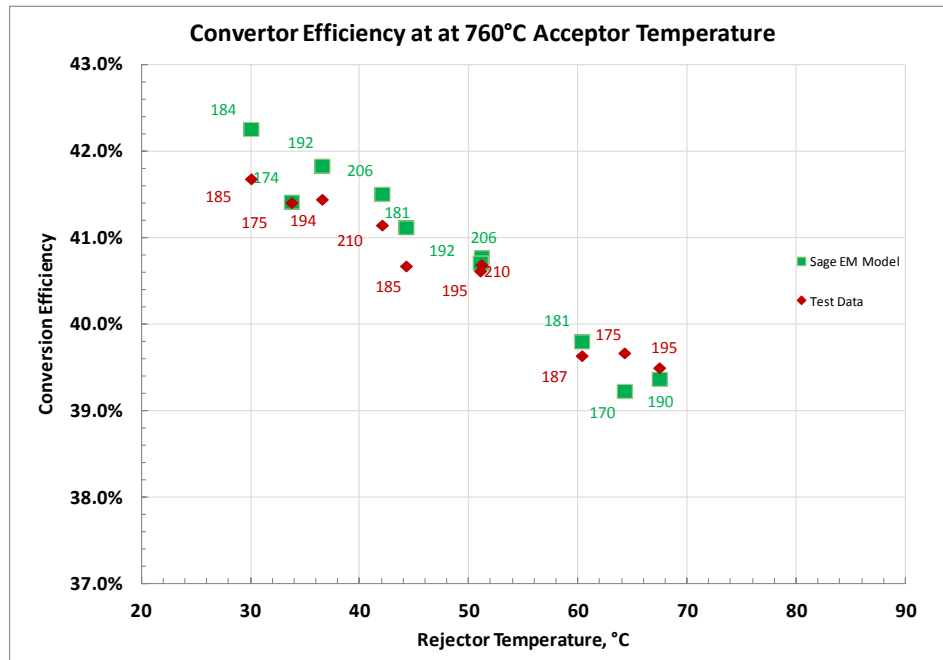


Figure 16: Sage ASC Model with EM Alternator, Comparison of Convertor Efficiency

Figure 17 compares power output of the EM model simulations against test data. The model agreed well with the test data at low reject temperatures, but the difference increases with increasing rejector temperature. This indicates that the model may not accurately account for temperature effects in the alternator, such as reduced magnetic saturation in the iron core or reduced magnet strength with increasing temperature. Even at high rejection temperature though, the model still agreed with test data within 5 percent.

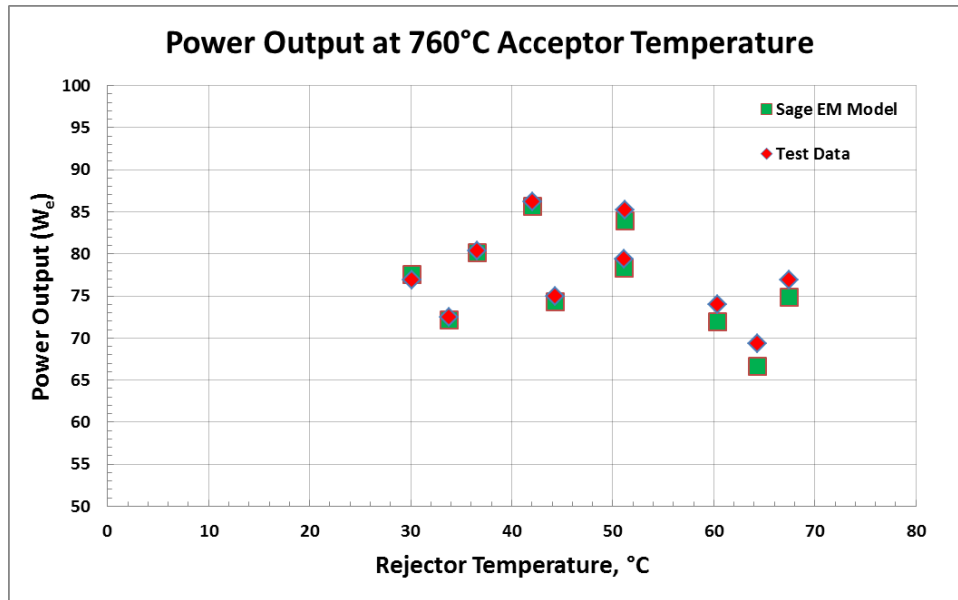


Figure 17: Sage ASC Model with EM Alternator, Comparison of Power Output

C. Sage Alternator Model Comparison

Figure 18 compares converter efficiency the Sage transducer model and EM model of the alternator against each other at their default (un-tuned) and tuned configurations when simulated at the BOM/EOM operating points. The default EM alternator model matches the data better than the default transducer model and almost as well as the tuned models. A plot displaying model comparison of power output (Fig. 19) shows similar results, though it should be noted that other parameters such as voltage, current, and power factor vary more in the default models (up to 20% error in the un-tuned models).

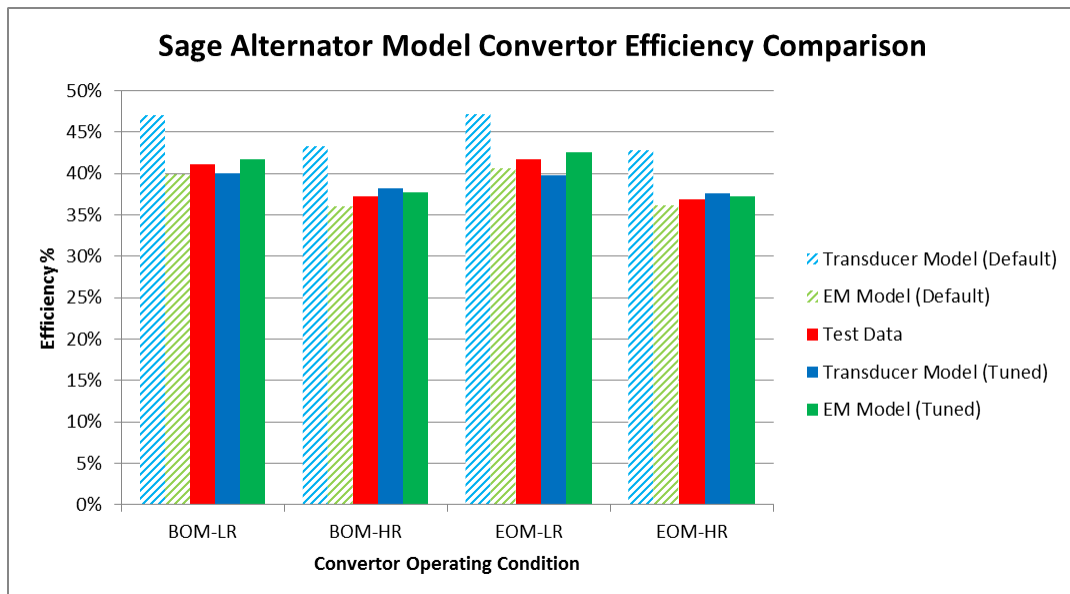


Figure 18: Sage Alternator Model Comparison of Converter Efficiency

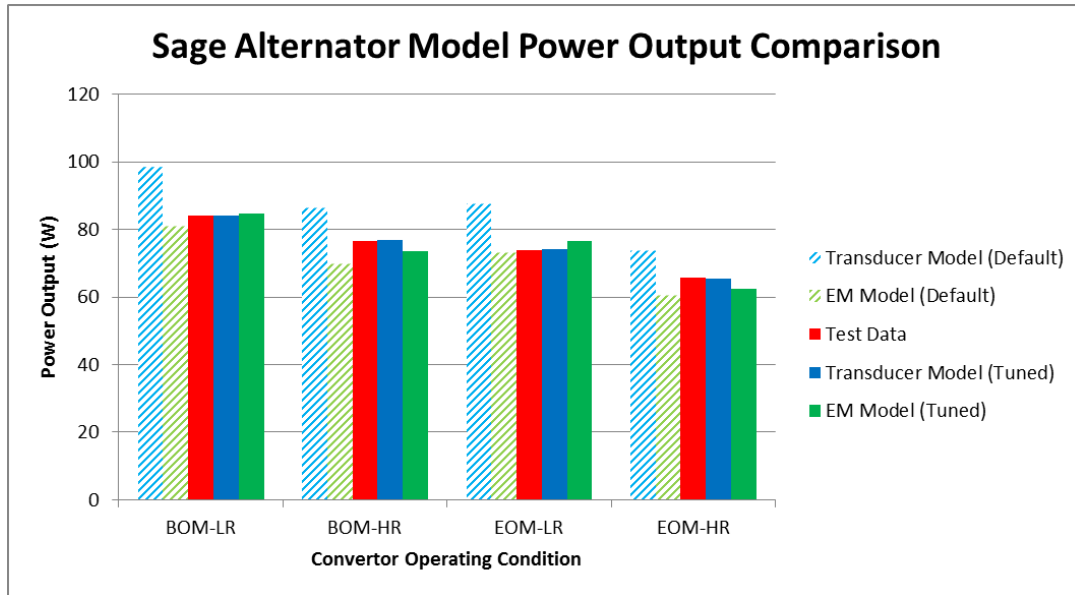


Figure 19: Sage Alternator Model, Power Output Comparison

IV. Conclusion

Two methods of modeling a linear alternator using the Sage 1-D modeling software were presented and used to create a more complete system model of the ASC. The models were tuned to BOM/EOM operating conditions using Sunpower data and simulation results were within about 5% of measured ASC performance. The models were then used in a performance mapping simulation and agreed with separate test data gathered at GRC within 5%. The transducer alternator model is the simpler model to implement but requires test data over a range of operating points to determine appropriate motor constant and loss parameters. The EM model is created from physical parameters of the alternator and does not require test data to perform preliminary simulations. This enables the EM model to be useful in the design of alternators as well as being able to tune it to test data. Using the Sage software to create a 1-D whole converter model of the ASC allow for simulations of steady-state converter performance without the more computationally intensive 3-D models.

Acknowledgments

This work was funded with the support of the NASA Science Mission Directorate and the Radioisotope Power Systems Program Office. Any opinions, findings, conclusions, or recommendations expressed in this article are those of the authors and do not necessarily reflect the views of NASA.

References

- ¹Thieme, Lanny G., Jeffrey G. Schreiber, and Lee S. Mason. *Stirling technology development at NASA GRC*. National Aeronautics and Space Administration, Glenn Research Center, 2001.
- ²Richardson, R. and Chan, J., "Advanced Stirling Radioisotope Generator," Proceedings of NASA Science Technology Conference (NSTC 2007)
- ³Wood, J.G, and Carrol, Cliff. "Advanced Stirling Converter Program Update," in *Proceedings of the Second International Energy Conversion Engineering Conference (IECEC 2004)* American Institute for Aeronautics and Astronautics, 2004.
- ⁴Wong, W.A., Wilson, K., Smith, E., and Collins, J. "Pathfinding the Flight Advanced Stirling Converter Design with the ASC-E3," in *Proceedings of the Tenth International Energy Conversion Engineering Conference (IECEC 2012)* American Institute for Aeronautics and Astronautics, 2012.
- ⁵Williams, Zachary D., and Oriti, Salvatore M. "Advanced Stirling Converter (ASC-E2) Characterization Testing," in *Proceedings of the Tenth International Energy Conversion Engineering Conference (IECEC 2012)* American Institute for Aeronautics and Astronautics, 2012.

- ⁶Oriti, Salvatore M. "Performance Measurement of Advance Stirling Convertors (ASC-E3)," in *Proceedings of the Eleventh International Energy Conversion Engineering Conference (IECEC 2013)* American Institute for Aeronautics and Astronautics, 2013.
- ⁷Dyson, Rodger W., Scott D. Wilson, and Roy C. Tew. "Review of Computational Stirling Analysis Methods," in *Proceedings of the Second International Energy Conversion Engineering Conference (IECEC 2004)* American Institute for Aeronautics and Astronautics, 2004.
- ⁸Lewandowski, E.J., and Regan, T.F., "Overview of the GRC Stirling Convertor System Dynamic Model," in *Proceedings of the Second International Energy Conversion Engineering Conference (IECEC 2004)*, American Institute of Aeronautics and Astronautics, 2004.
- ⁹Ebiana, A. B., Savadekar, R.T., Vallury, A. "2nd Law Analysis of Sage and CFD-ACE+ Models of MIT Gas Spring and "Two-Space" Test Rigs," in *Proceedings of the Second International Energy Conversion Engineering Conference (IECEC 2004)* American Institute for Aeronautics and Astronautics, 2004.
- ¹⁰Zhang, Zhiguo and Ibrahim, Mounir. "Development of CFD model for Stirling Engine and its Components," in *Proceedings of the Second International Energy Conversion Engineering Conference (IECEC 2004)* American Institute for Aeronautics and Astronautics, 2004.
- ¹¹Dyson, Rodger W., Wilson, Scott D., Tew, Roy C., and Demko, R. "On the Need for Multidimensional Stirling Simulations," in *Proceedings of the Third International Energy Conversion Engineering Conference (IECEC 2005)* American Institute for Aeronautics and Astronautics, 2005.
- ¹²Geng, Steven M., and Schwarze, Gene E. "A 3-D Magnetic Analysis of a Linear Alternator for a Stirling Power System," in *Proceedings of the 36th Intersociety Energy Conversion Engineering Conference (IECEC 2001)*, Savannah, GA, 2001.
- ¹³Gedeon, David. "Sage: Object Oriented Software for Stirling Machine Design," AIAA Paper 94-4106-CP. 1994.
- ¹⁴Gedeon, David. "Sage User's Guide, Ninth Edition," Gedeon Associates, 2013.
- ¹⁵Griffiths, D.J., *Introduction to Electrodynamics*, Prentice Hall, New Jersey, 1989.
- ¹⁶Halliday, David, and Resnick, Robert, *Fundamentals of Physics*, 2nd ed., John Wiley & Sons, New York, 1986, Chaps.32-34.
- ¹⁷Reitz, J.R., Milford, F.J, and Christy, R.W., *Foundations of Electromagnetic Theory*, 3rd ed., Addison-Wesley Publishing Company, Inc., Reading, MA, 1980, Chaps. 9-12.
- ¹⁸Metscher, Jonathan F., and Lewandowski, Edward J. "Development and Integration of an Advanced Stirling Convertor Linear Alternator Model for a Tool Simulating Convertor Performance and Creating Phasor Diagrams," in *Proceedings of the Eleventh International Energy Conversion Engineering Conference (IECEC 2013)* American Institute for Aeronautics and Astronautics, 2013.